Physics 140A-Introduction to Solid State Physics
Winter, 2016
Problem Set 3
Due Thursday, 18 February

Reading: Finish Omar, Chapter 2, Read Chapter 3 on Lattice Vibrations, Sections 3.1-3.10
Plus supplemental reading from Kittel on Debye-Waller factors
Diffraction:
(Questions and Problems in Omar from Chapter 2 indicated as 2.x)

[1] Question 2.1
[2] Question 2.2 (We discussed this in lecture.)
[3] Question 2.3
[4] Problem 2.3.
[5] Problem 2.6. A hint here is to let the vector s lie along the z direction in spherical polar coordinates, which simplifies the integration greatly.
[6] Problem 2.8 (Also discussed in lecture in more detail.)
[7] Problem 2.9. Hint: You can let the limit on the integral R go to infinity, since the hydrogen wave function dies off quickly in r due to the exponential in its charge density.
[8] Problem 2.13
[9] Problem 2.19, plus as an additional part show the Ewald construction for diffraction of 10.0 keV x-rays incident on this 2D crystal along the direction of the basis vector $\vec{a}$, and comment on whether any diffraction spots would be observed.
[10] Problem 2.20,
(d) Reword as: A general formula for the Bragg angle for reflection from the above (210) planes.
Plus additional special part as:
(e) Show with one or more cross-sections and/or 3D sketches what the first Brillouin zone would look like for this unit cell.
[11] Problem 2.25

Some diffracting waves/de Broglie waves

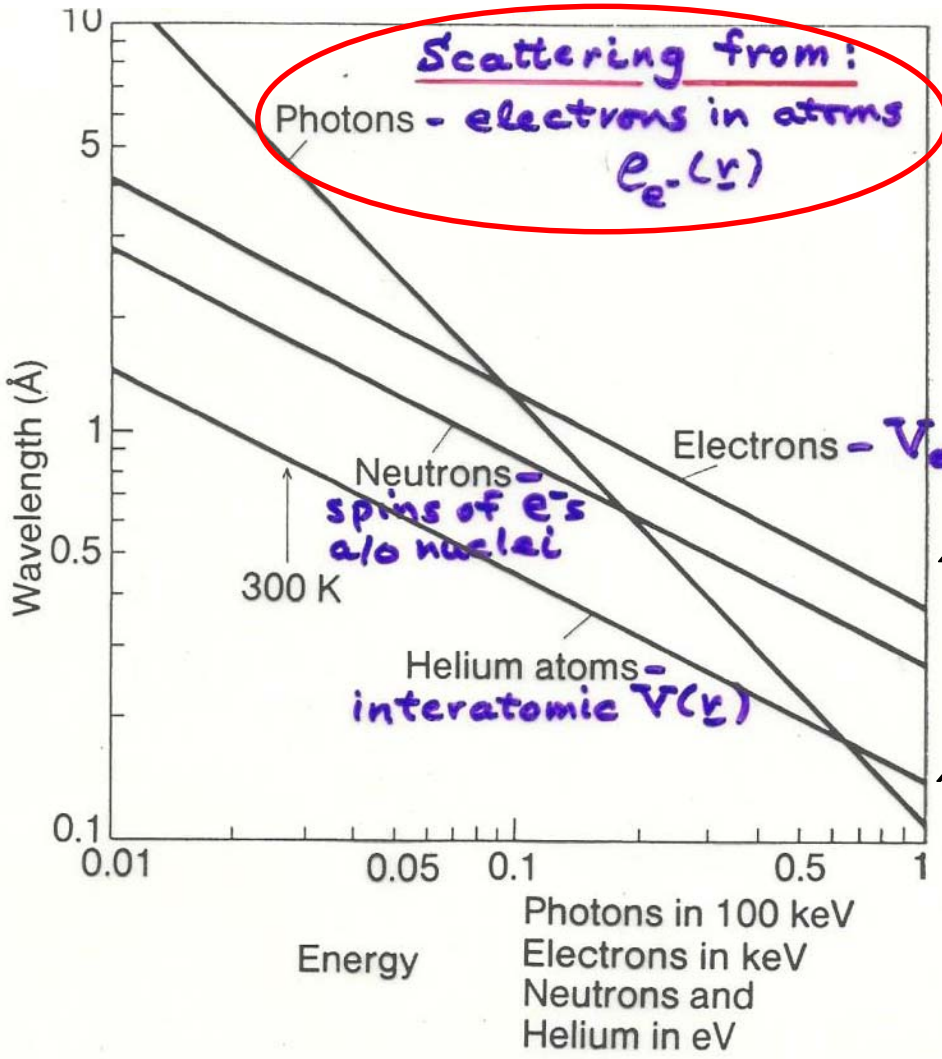

$$\lambda_x = \frac{12,400}{h\nu\ (eV)}$$

$$\lambda_e = \frac{h}{p} = \frac{h}{\sqrt{2m_e E_{kin}}} = \sqrt{\frac{150}{E_{kin}\ (eV)}}$$

$$\lambda_n = \frac{h}{p} = \frac{0.28}{\sqrt{E_{kin}\ (eV)}}$$

$$\lambda_{He} = \frac{h}{p} = \frac{0.14}{\sqrt{E_{kin}\ (eV)}}$$

The generation of x-rays:

An x-ray tube:

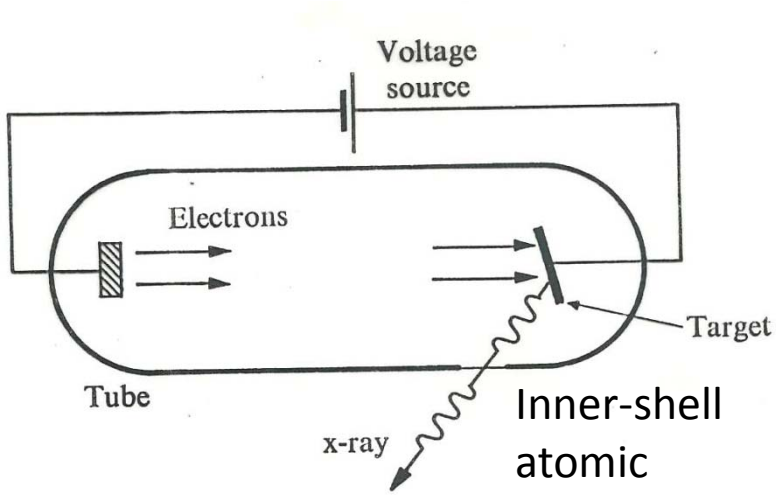

Inner-shell atomic transitions

Synchrotron radiation: e.g. the Berkeley Advanced Light Source

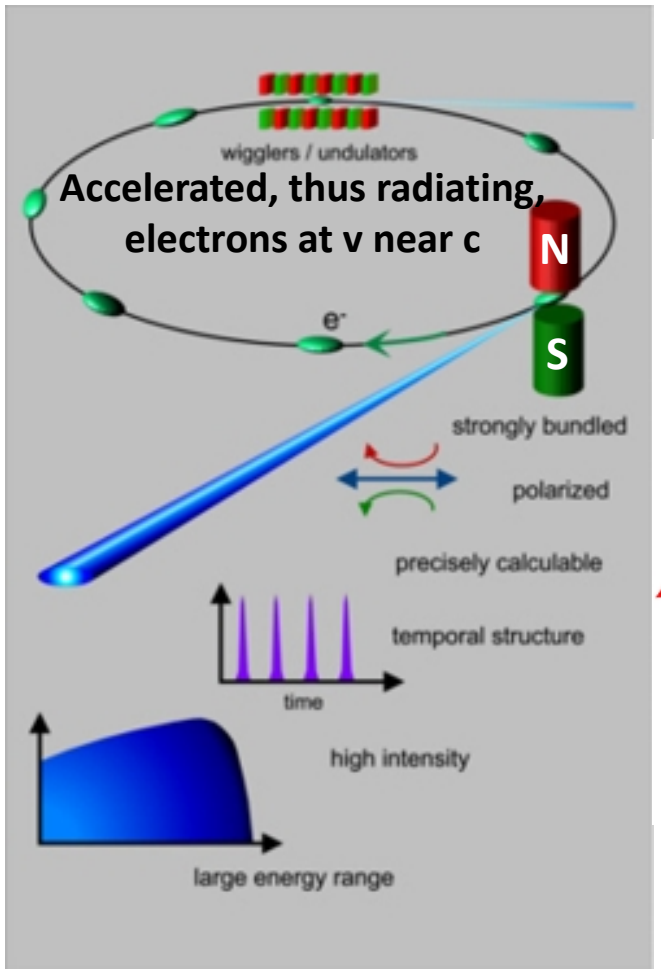

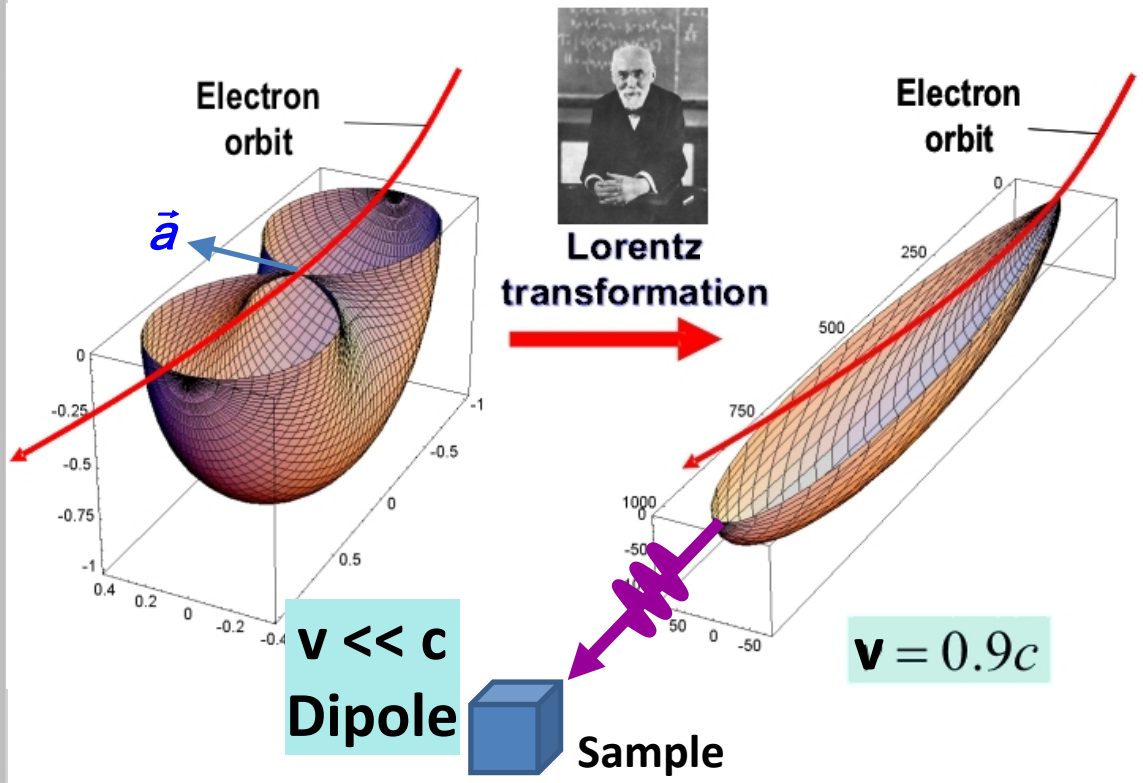

The five ways in which x-rays interact with matter:

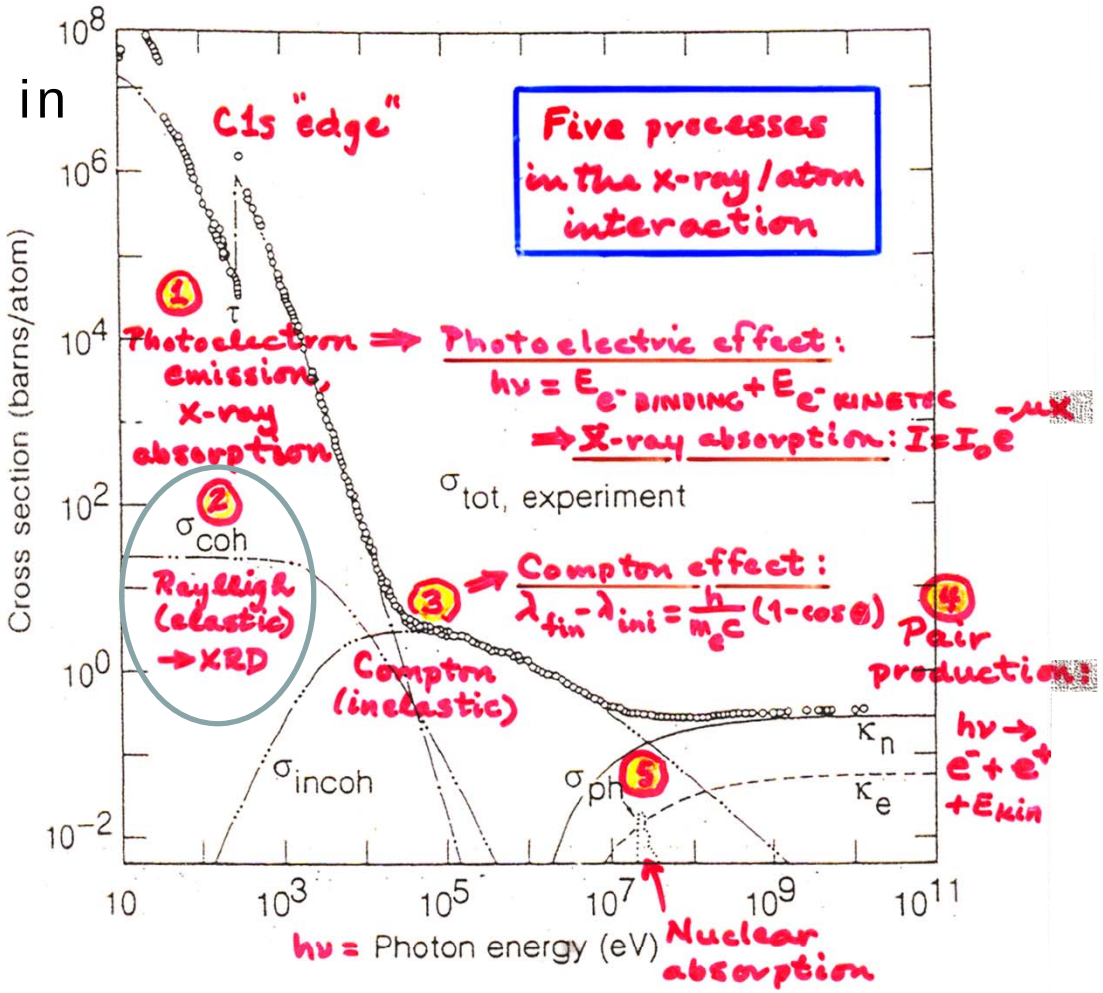

Fig. 3-1. *Total photon cross section σ_{tot} in carbon, as a function of energy, showing the contributions of different processes: τ, atomic photo-effect (electron ejection, photon absorption); σ_{coh}, coherent scattering (Rayleigh scattering—atom neither ionized nor excited); σ_{incoh}, incoherent scattering (Compton scattering off an electron) κ_n, pair production, nuclear field; κ_e, pair production, electron field; σ_{ph}, photonuclear absorption (nuclear absorption usually followed by emission of a neutron or other particle). (From Ref. 3; figure courtesy of J. H. Hubbell.)*

LBNL Center for X-Ray Optics
"X-Ray Data Booklet"
Section 3.1
http://cxro.lbl.gov/x-ray-data-booklet

Bragg's Law and crystal planes

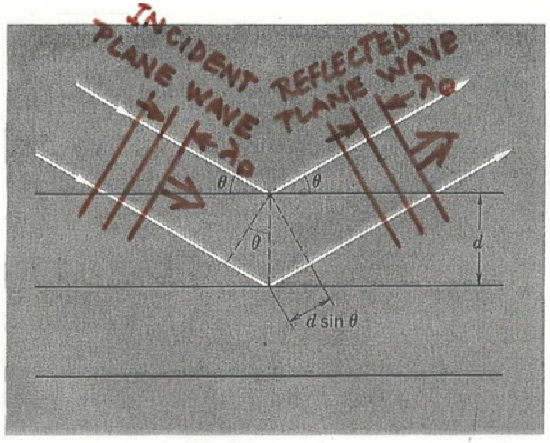

Figure 2 Derivation of the Bragg equation $2d \sin\theta = n\lambda$; here d is the spacing of parallel atomic planes and $2n\pi$ is the difference in phase between reflections from successive planes. What do we mean by a set of parallel reflecting planes? Any set of parallel planes will do, provided each plane passes through at least three non-colinear lattice points! See Fig. 3 for several examples. *The reflecting planes have nothing to do with the surface planes bounding the particular specimen,* because the x-rays or neutrons see all!

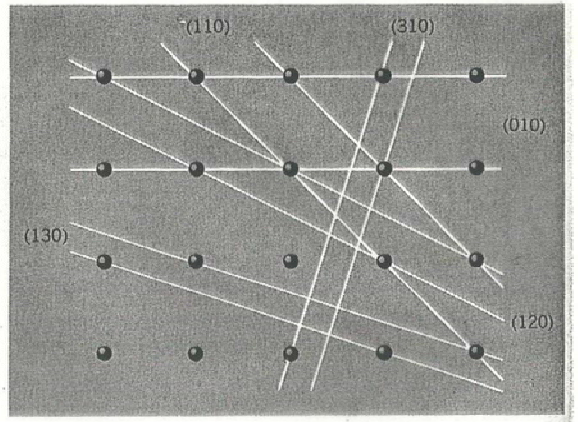

Figure 3 Several types of reflecting planes in a simple cubic crystal lattice. The planes shown are labeled by their Miller indices. We have shown in each case a set of two parallel planes. The closest distance between parallel planes tends to decrease as the indices increase; thus high index reflections require shorter wavelengths. In principle the number of different types of reflecting planes is unlimited if the crystal is infinite.

CONSTRUCTIVE INTERFERENCE BETWEEN PLANES FOR:

$$\boxed{n\lambda_0 = 2d_{hkl} \sin\theta}$$ — BRAGG'S LAW

n: 1,2,3,...

$\lambda_0 \leq 2d$

Basics of scattering from individual electrons

Unit vectors

$k \equiv |\bar{k}_0| = |\bar{k}|$: ELASTIC SCATT.

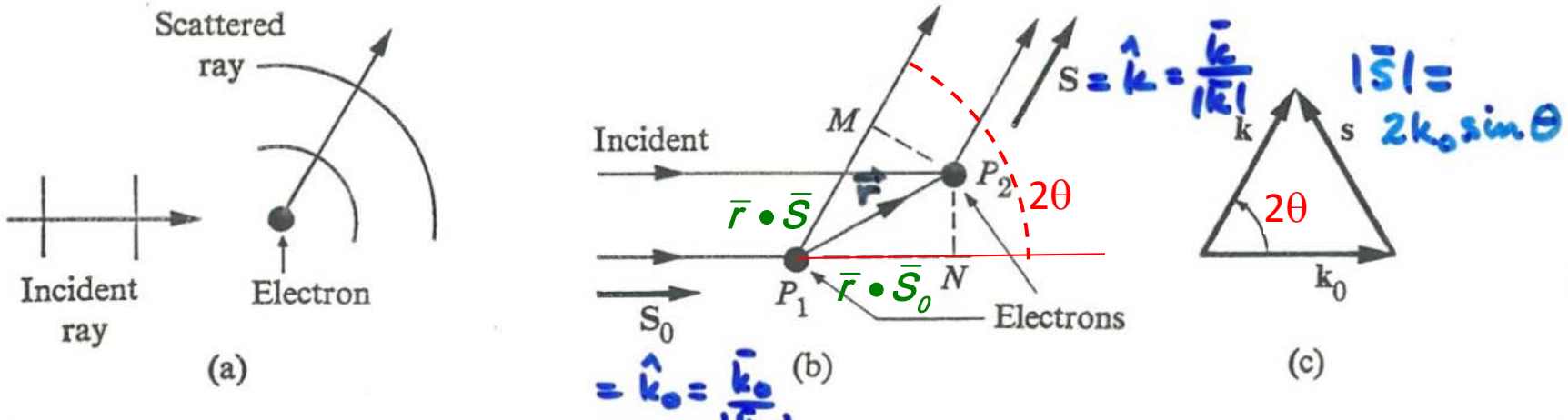

Fig. 2.3 Scattering from (a) a single electron, (b) two electrons. (c) The scattering vector s. Note that the vectors $\mathbf{k}_0$, $\mathbf{k}$, and $\mathbf{s}$ form an isosceles triangle.

PHASE DIFFERENCE DUE TO :
PATH LENGTH VIA P_1 – PATH LENGTH VIA P_2

$$L = \bar{r}\cdot\bar{S} - \bar{r}\cdot\bar{S}_0 \equiv \bar{r}\cdot\hat{k} - \bar{r}\cdot\hat{k}_0 \equiv \bar{r}\cdot(\hat{k}-\hat{k}_0) \equiv \bar{r}\cdot\bar{s}/k$$

$$\text{PHASE DIFF.} = \delta = \bar{s}\cdot\bar{r}$$

SCATTERING VECTOR

Scattering from an arbitrary electron charge distribution

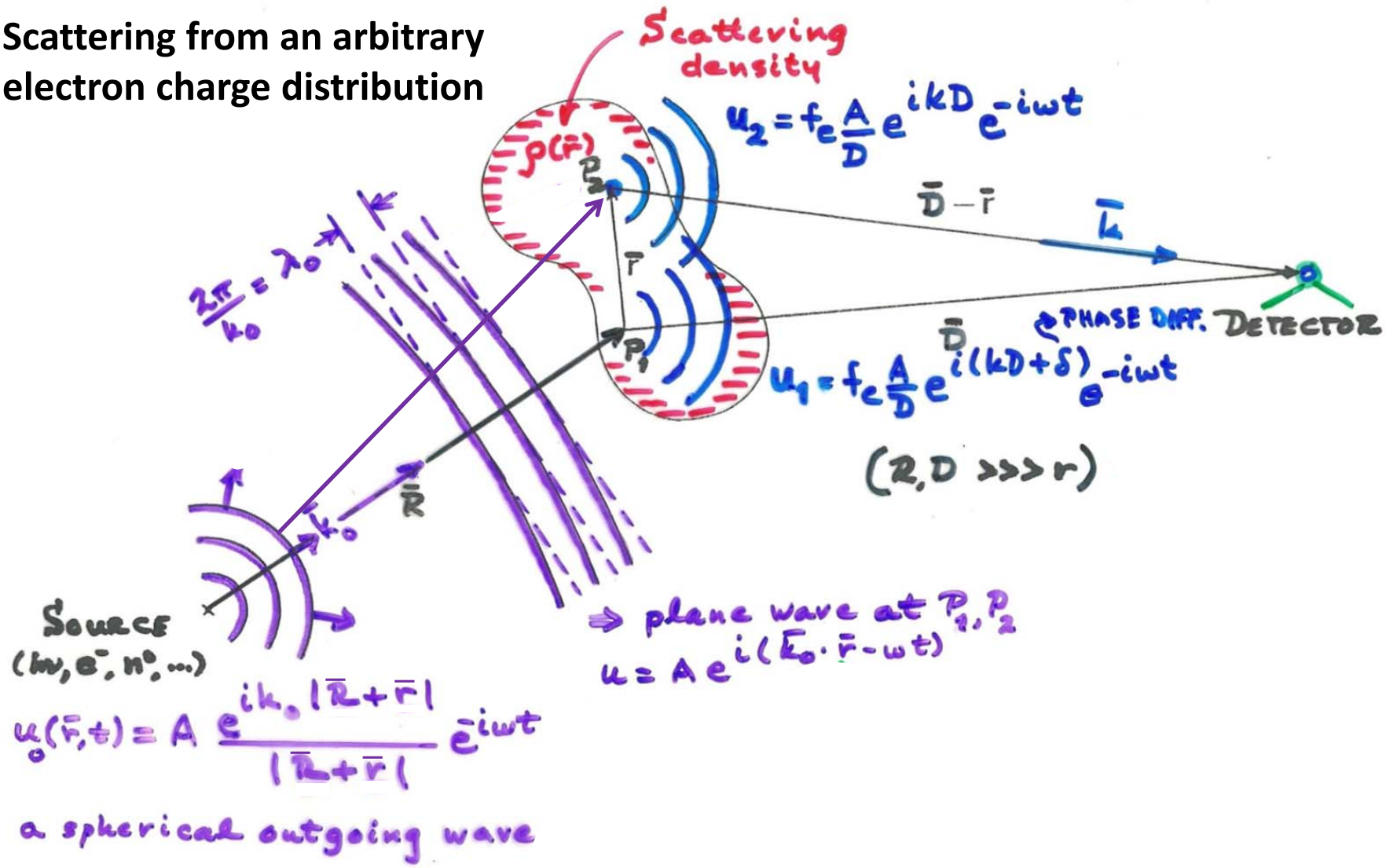

Scattering from an arbitrary electron charge distribution

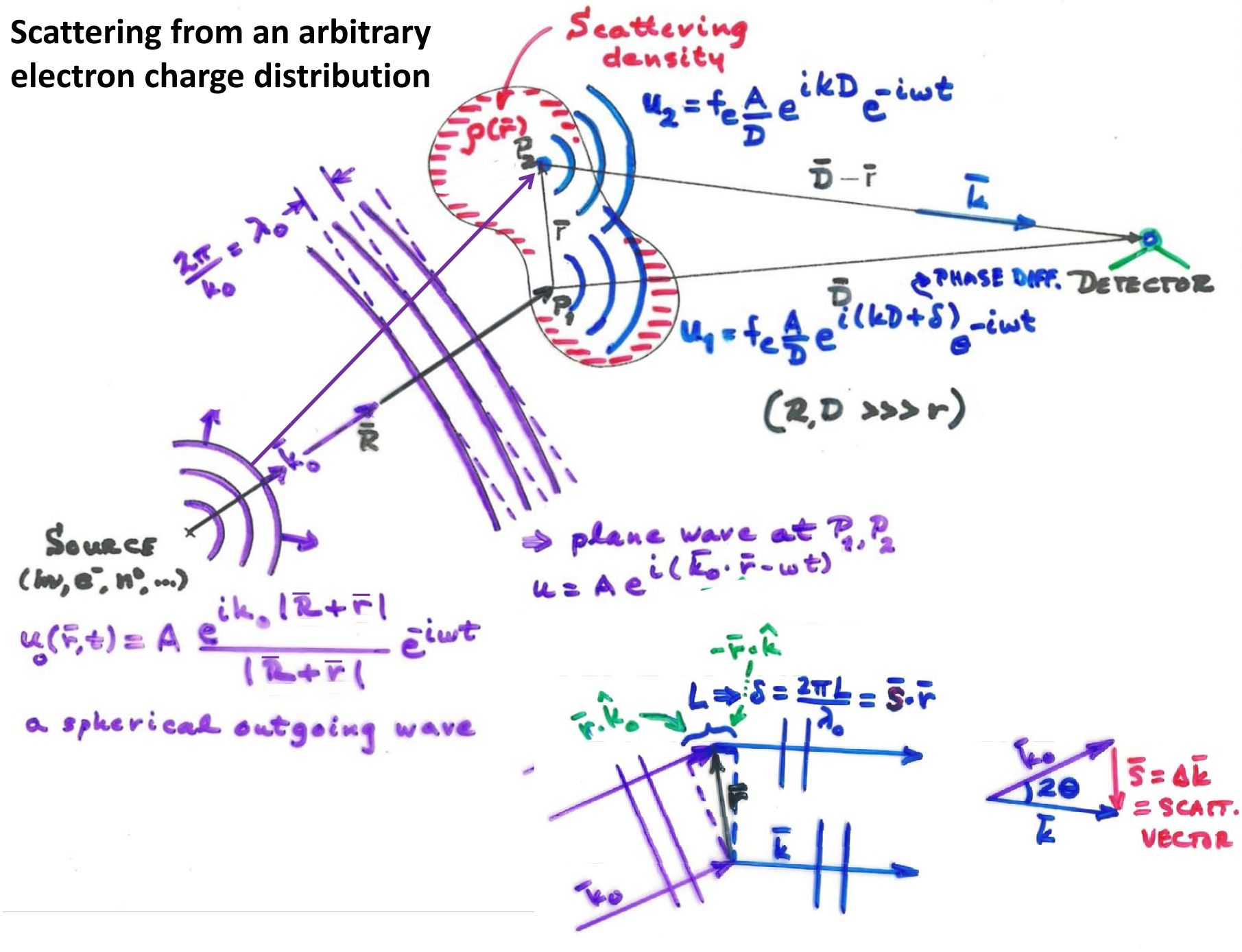

Scattering from an arbitrary electron charge distribution

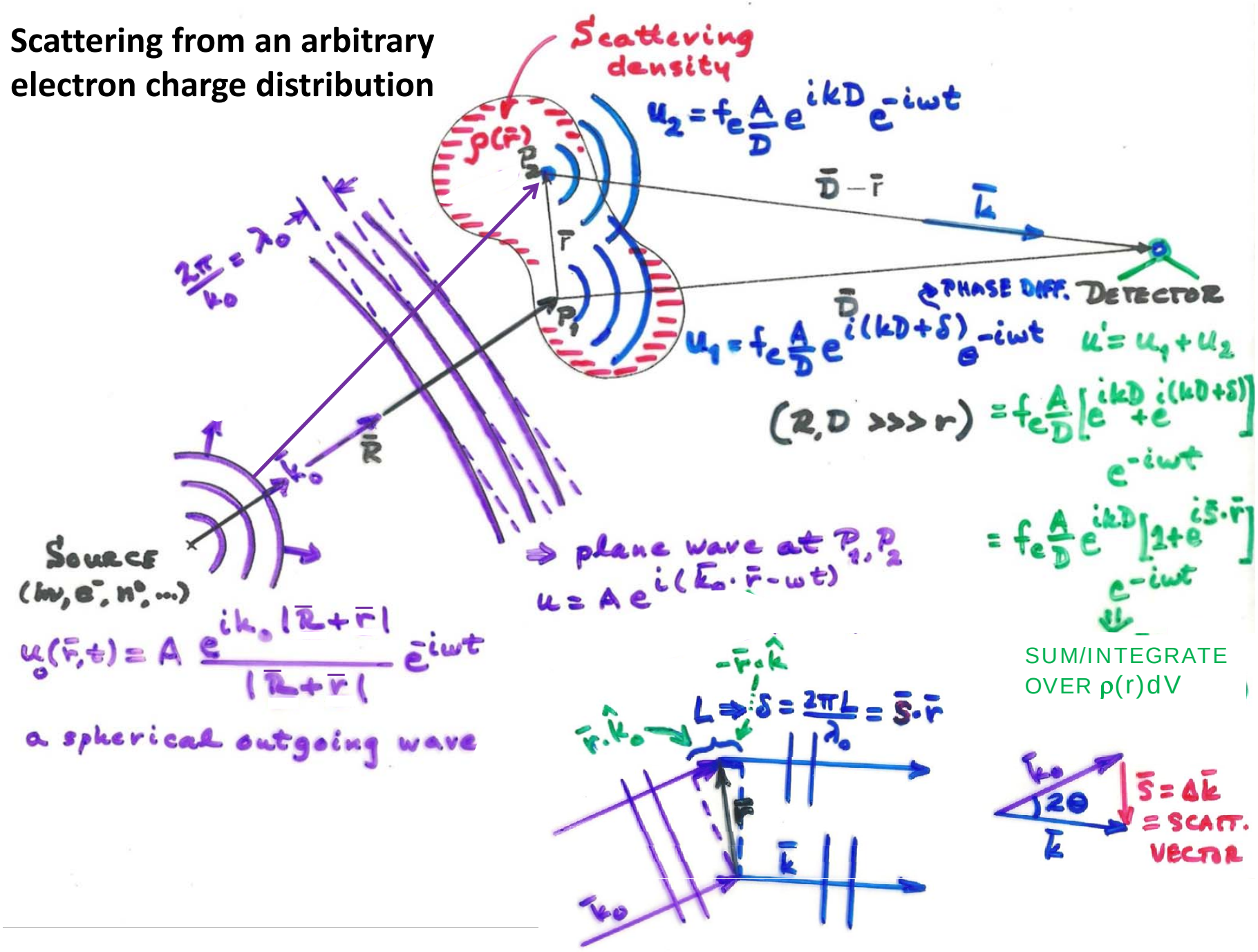

Scattering from a single atom: spherically symmetric charge distribution

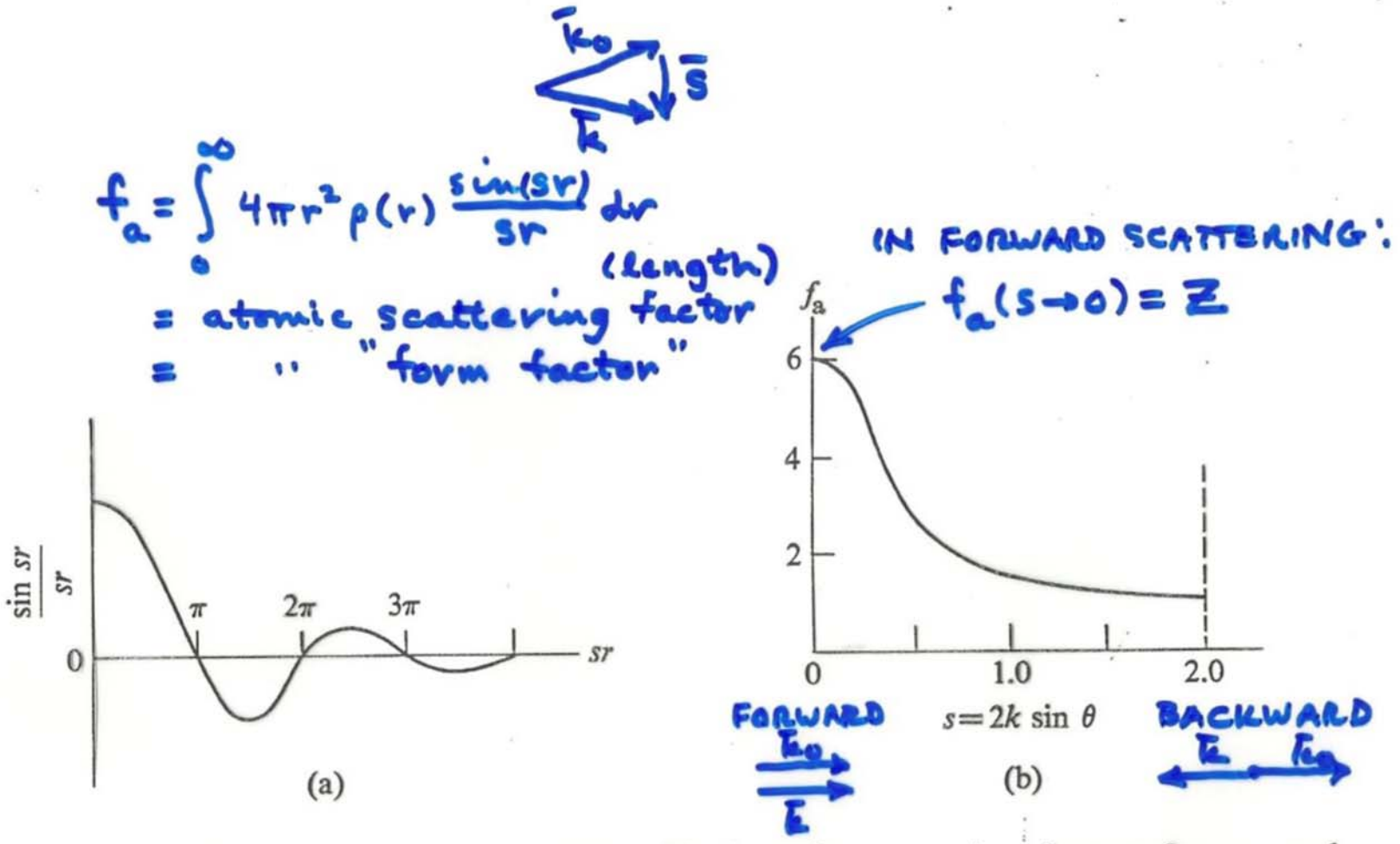

Fig. 2.4 (a) Oscillating factor $\sin(sr)/sr$. (b) Atomic scattering factor for a carbon atom as a function of the scattering angle (after Woolfson).

An atomic scattering (form) factor

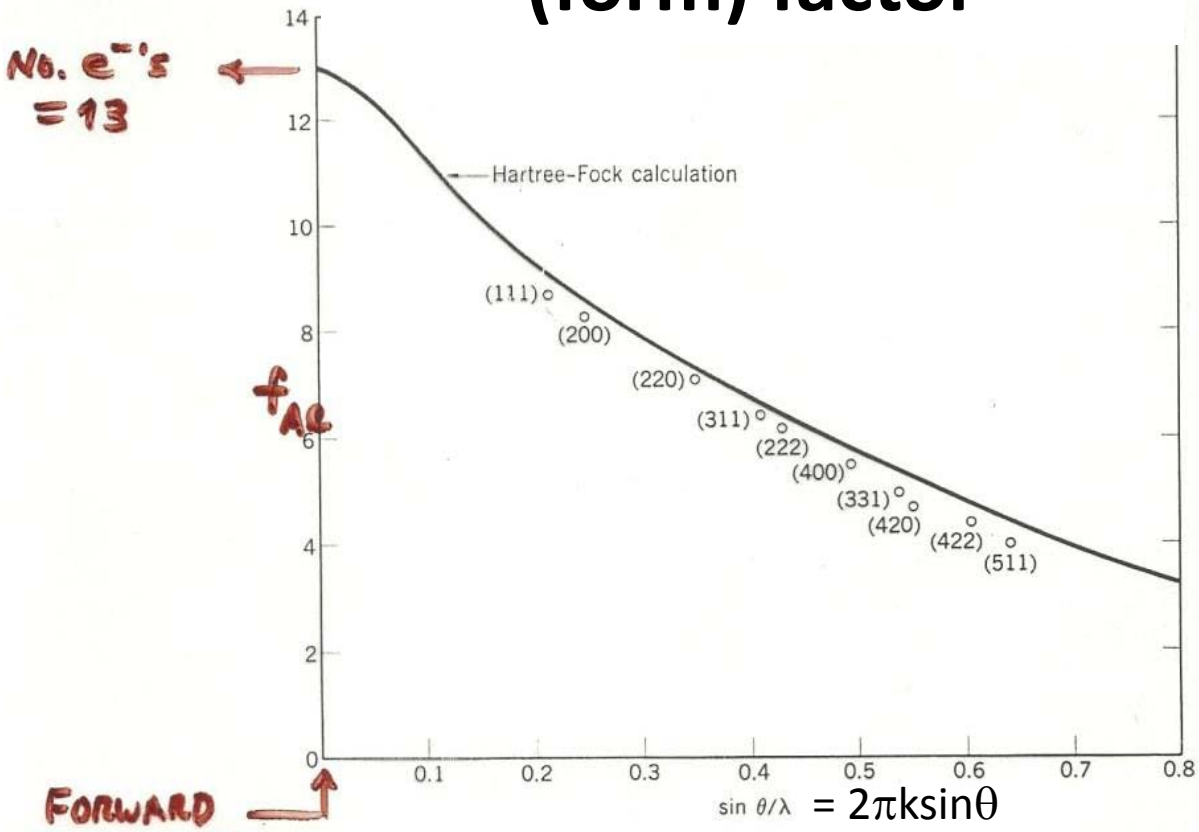

Figure 32 Absolute experimental atomic scattering factors for metallic aluminum, after Batterman, Chipman, and DeMarco. Each observed reflection is labeled. The incident radiation was MoKα with λ = 0.709 Å. Note that no reflections occur for which the indices are partly even and partly odd; this is what we expect for an fcc crystal, according to (63).

Diffraction from a linear chain of point scatterers

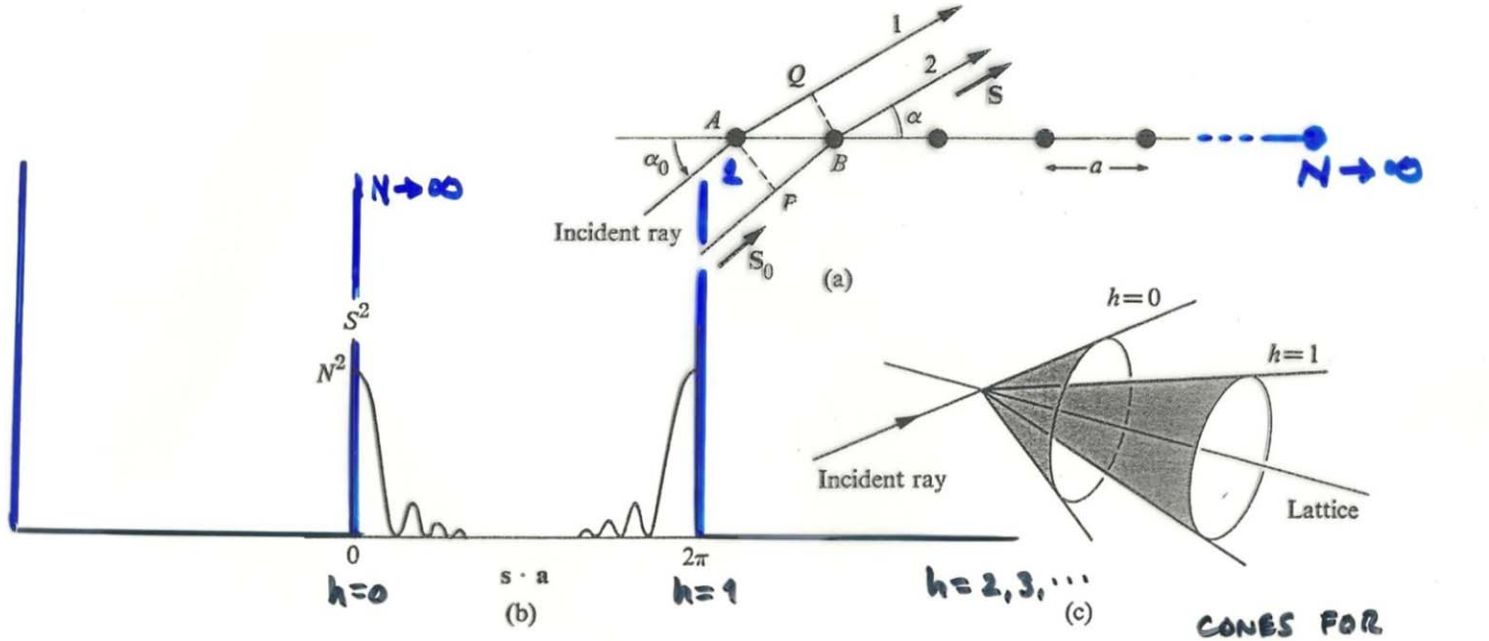

CONES FOR

$\bar{s}\cdot\bar{a} = 2\pi h$

$h = 1, 2, 3, \ldots$

$$I \propto S^2 = \left| \sum_{\ell=1}^{N} e^{i\bar{s}\bullet\ell\bar{a}} \right|^2 = \frac{\sin^2\left[\left(\frac{1}{2}\right)N\bar{s}\bullet\bar{a}\right]}{\sin^2\left[\left(\frac{1}{2}\right)\bar{s}\bullet\bar{a}\right]}$$

EQUIVALENT TO:

$\frac{2\pi a}{\lambda}(\cos\alpha - \cos\alpha_0) = 2\pi h$

$\overline{AQ} - \overline{PB} = h\lambda$

Diffraction from a crystal with a basis

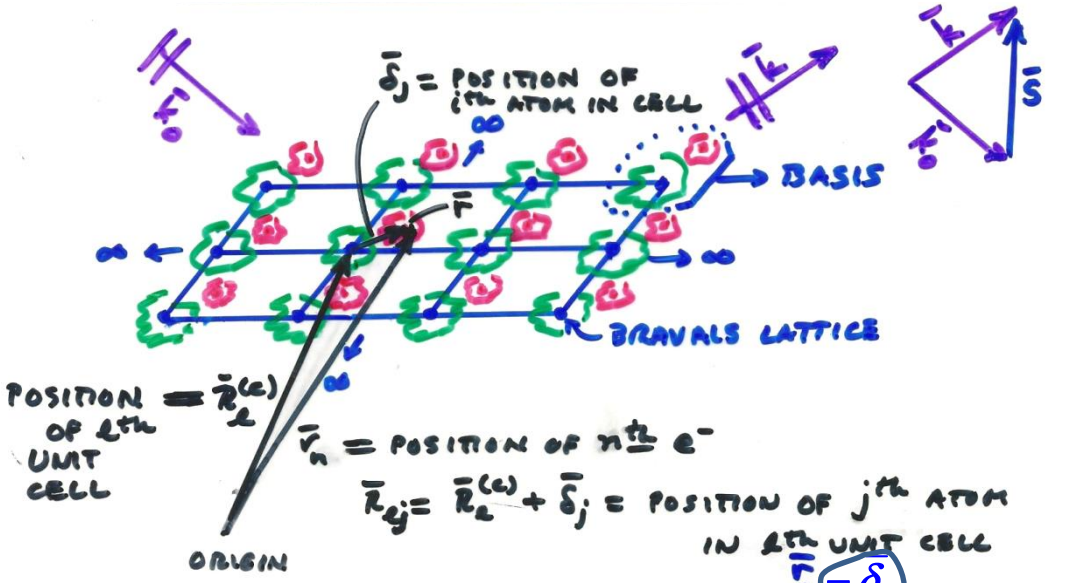

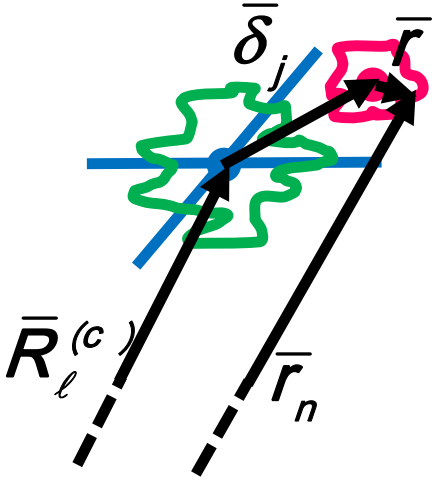

$$f_{Cryst} = \sum_{n}^{(\text{ALL } e^-\text{S})} e^{i\bar{s}\cdot\bar{r}_n} = \sum_{\ell j}\left(\int_{0}^{r_{ATOM}} \rho_{aj}(\bar{r}) e^{i\bar{s}\cdot[\bar{r}_n - \bar{R}_{\ell j}]} d^3r\right)\cdot e^{i\bar{s}\cdot\bar{R}_{\ell j}}$$

$\bar{r} - \delta_j$

INTEGRATE OVER EACH ATOM

f_{aj} = ATOMIC SCATTERING FACTOR (LENGTH)

$$= \sum_{\ell j} f_{aj} e^{i\bar{s}\cdot\bar{\delta}_j} e^{i\bar{s}\cdot\bar{R}_\ell^{(c)}} = \underbrace{\sum_j f_{aj} e^{i\bar{s}\cdot\bar{\delta}_j}}_{\text{UNIT CELL}} \cdot \underbrace{\sum_{\ell} e^{i\bar{s}\cdot\bar{R}_\ell^{(c)}}}_{\text{ALL CELLS}}$$

$\bar{F}$ = GEOMETRIC STRUCT. FACTOR

$\bar{S}$ = LATTICE STRUCT. FACTOR

The Ewald construction for allowed diffraction

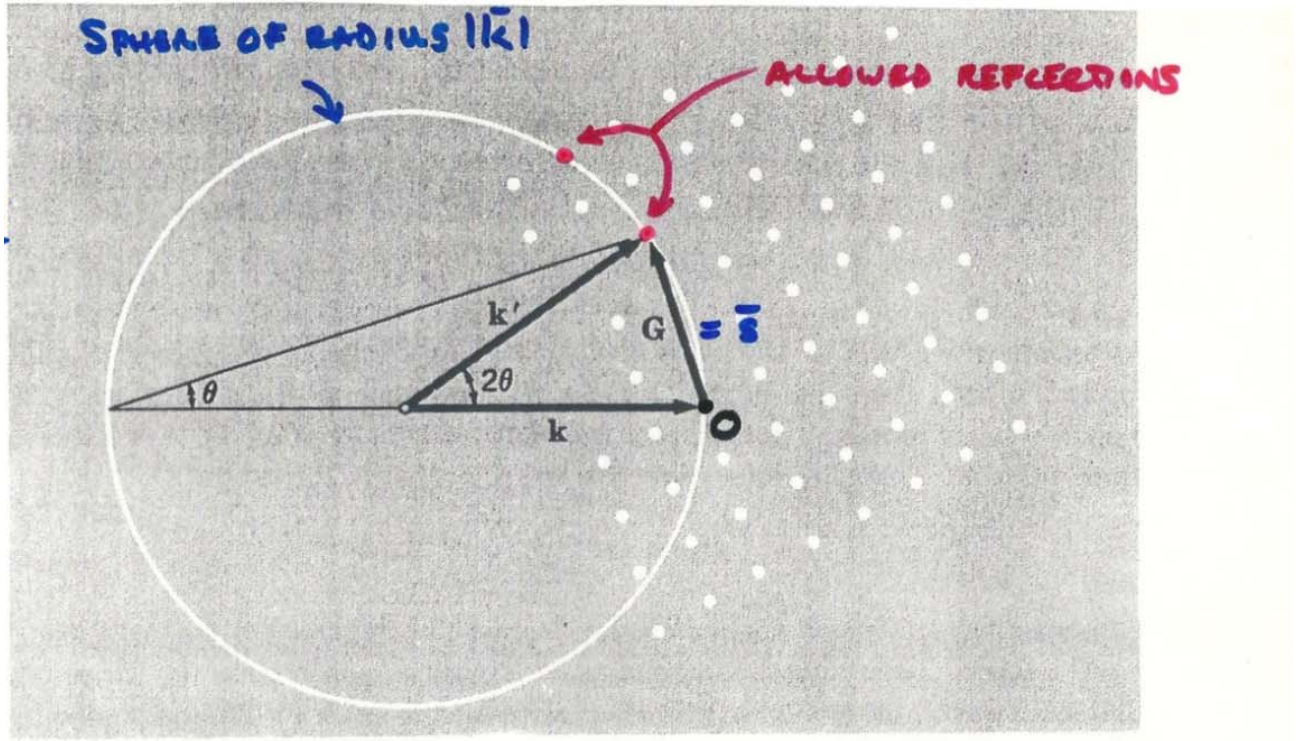

0b The points on the right-hand side are reciprocal lattice points of the crystal. The vector
vn in the direction of the incident x-ray beam and it terminates at any reciprocal lattice
e draw a sphere of radius $k = 2\pi/\lambda$ about the origin of **k**. A diffracted beam will be formed
here intersects any other point in the reciprocal lattice. The sphere as drawn intercepts a
nnected with the end of **k** by a reciprocal lattice vector **G**. The diffracted x-ray beam is in
tion $\mathbf{k}' = \mathbf{k} + \mathbf{G}$. This construction is due to P. P. Ewald.

The Unit Cell Structure Factor F and forbidden reflections

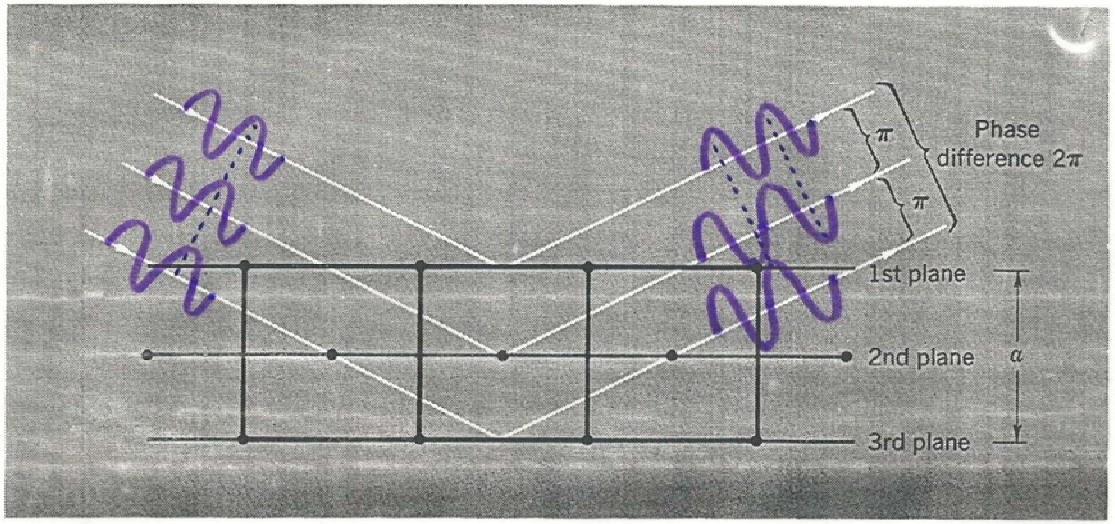

Figure 30 Explanation of the absence of a (100) reflection from a body-centered cubic lattice. The phase difference between successive planes is π, so that the reflected amplitude from two adjacent planes is $1 + e^{-i\pi} = 1 - 1 = 0$.

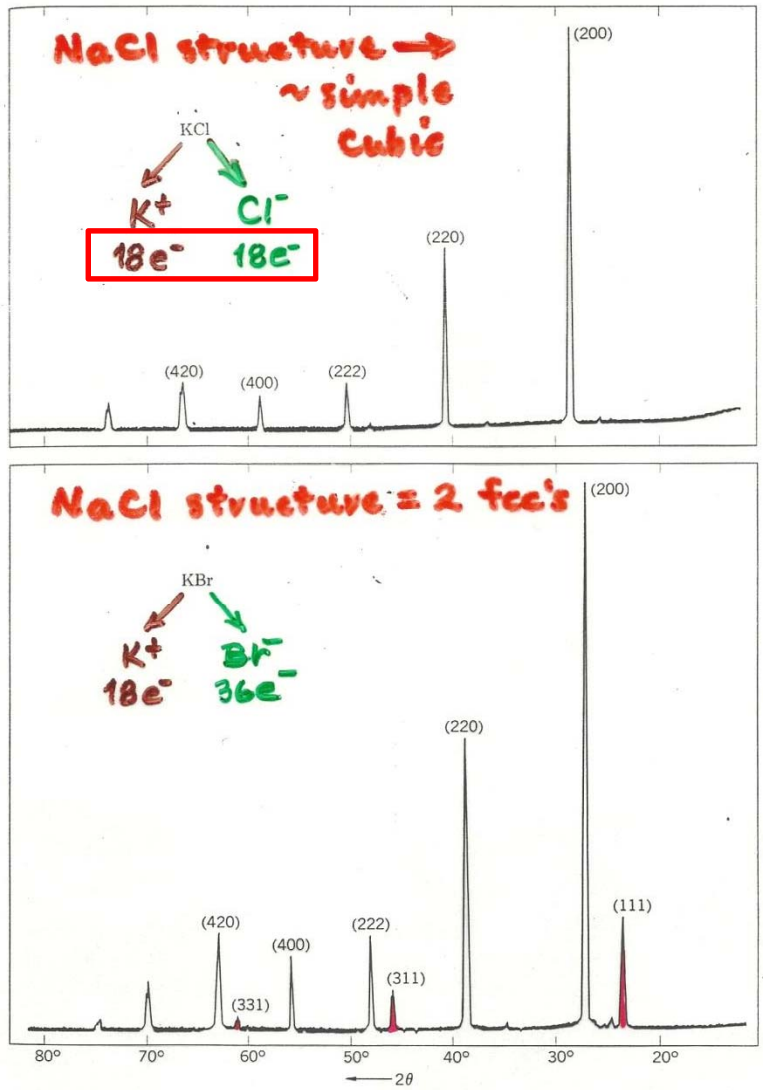

Figure 31 Comparison of x-ray reflections from KCl and KBr powders. In KCl the numbers of electrons of K^+ and Cl^- ions are equal. The scattering amplitudes $f(K^+)$ and $f(Cl^-)$ are almost exactly equal, so that the crystal looks to x-rays as if it were a monatomic simple cubic lattice of lattice of lattice constant $a/2$. Only even integers occur in the reflection indices when these are based on a cubic lattice of lattice constant a. In KBr the form factor of Br^- is quite different than that of K^+, and all reflections of the fcc lattice are present. (Courtesy of Robert van Nordstrand.)

Forbidden reflections

Brillouin zone for a simple 2D square lattice

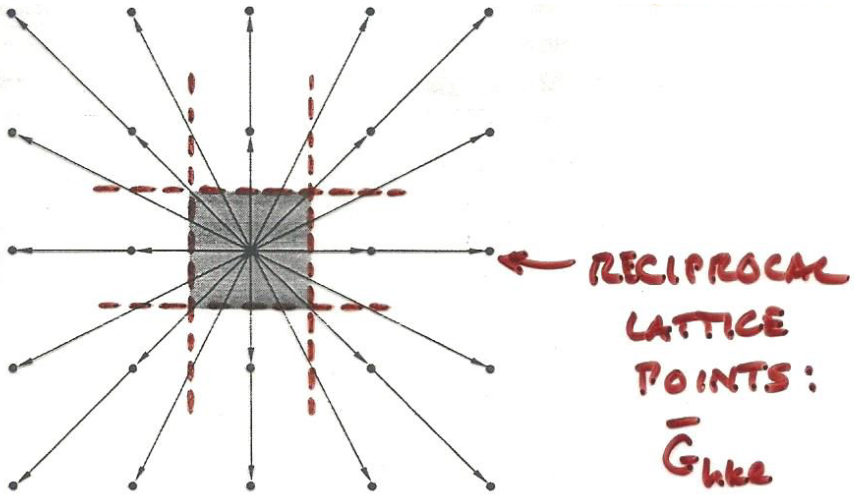

Figure 22 Square reciprocal lattice with reciprocal lattice vectors shown as fine black lines. The lines shown in white are perpendicular bisectors of the reciprocal lattice vectors. The central square is the smallest volume about the origin which is bounded entirely by white lines. The square is the Wigner-Seitz primitive cell of the reciprocal lattice.

1st Brillouin zone for the fcc lattice

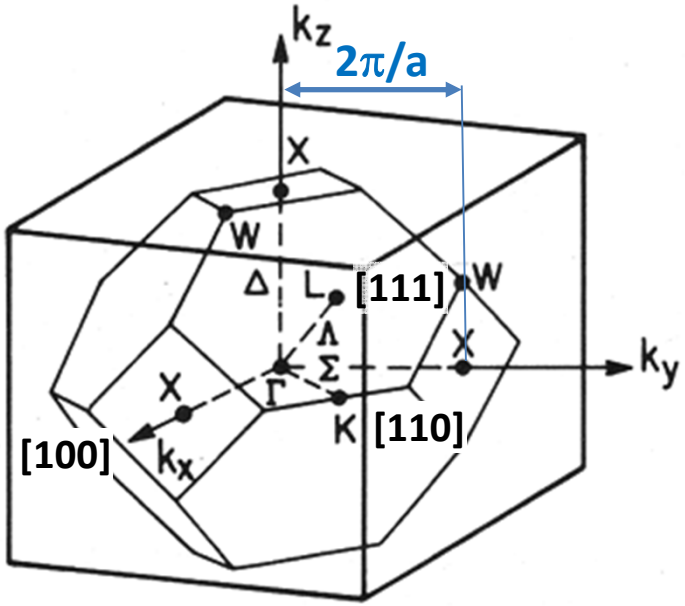

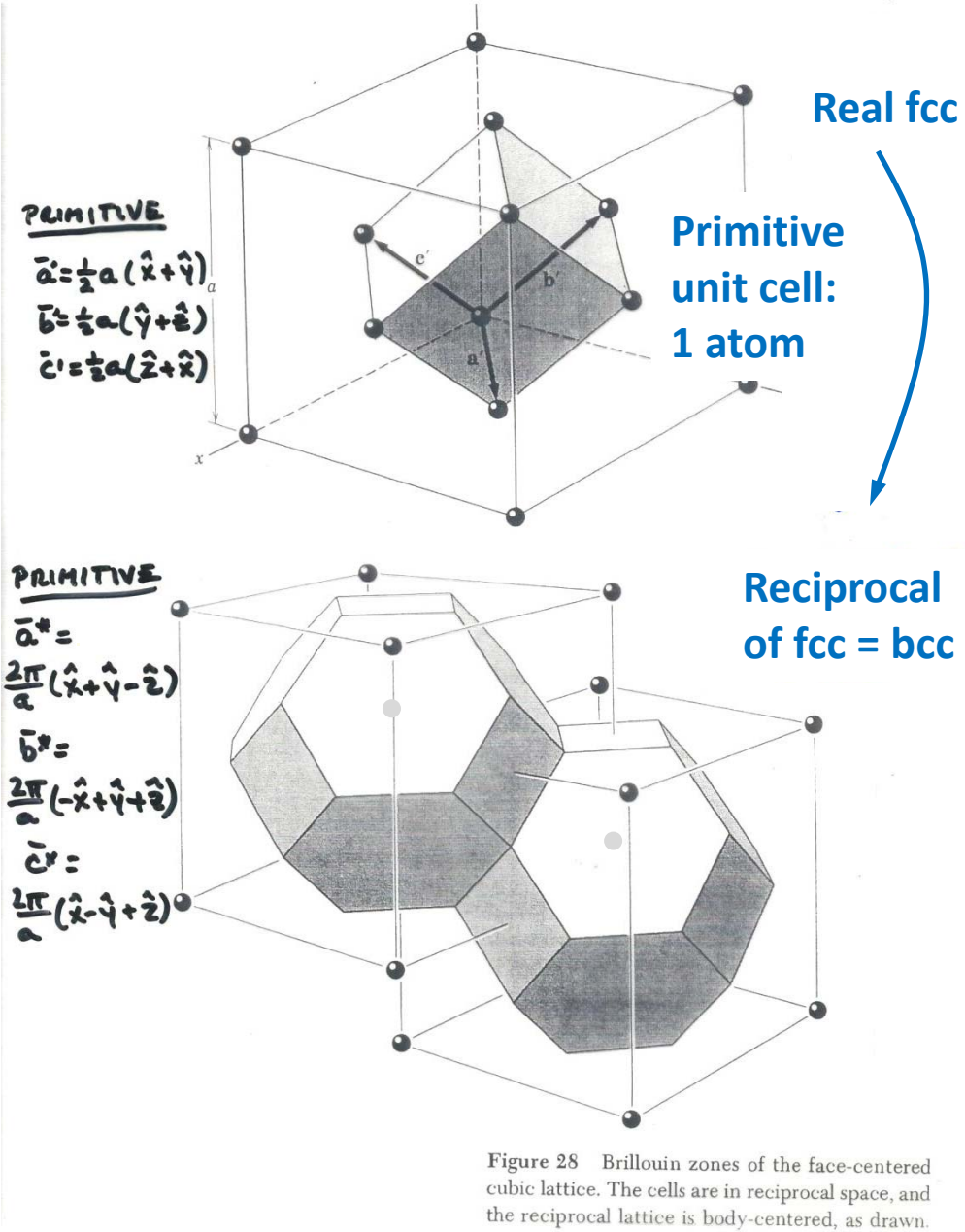

Figure 28 Brillouin zones of the face-centered cubic lattice. The cells are in reciprocal space, and the reciprocal lattice is body-centered, as drawn.

Electronic bands and density of states for a semiconductor-Germanium—
$1s^2 2s^2\ 2p^6 3s^2\ 3p^6 3d^{10} 4s^2 4p^2$

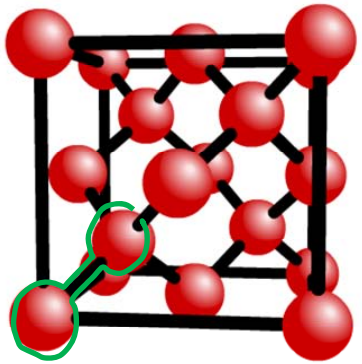

Diamond Structure
= fcc
+ 2-atom basis

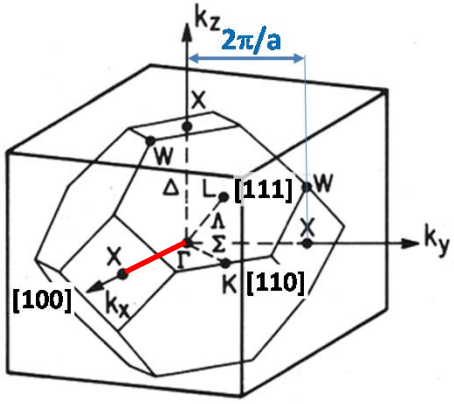

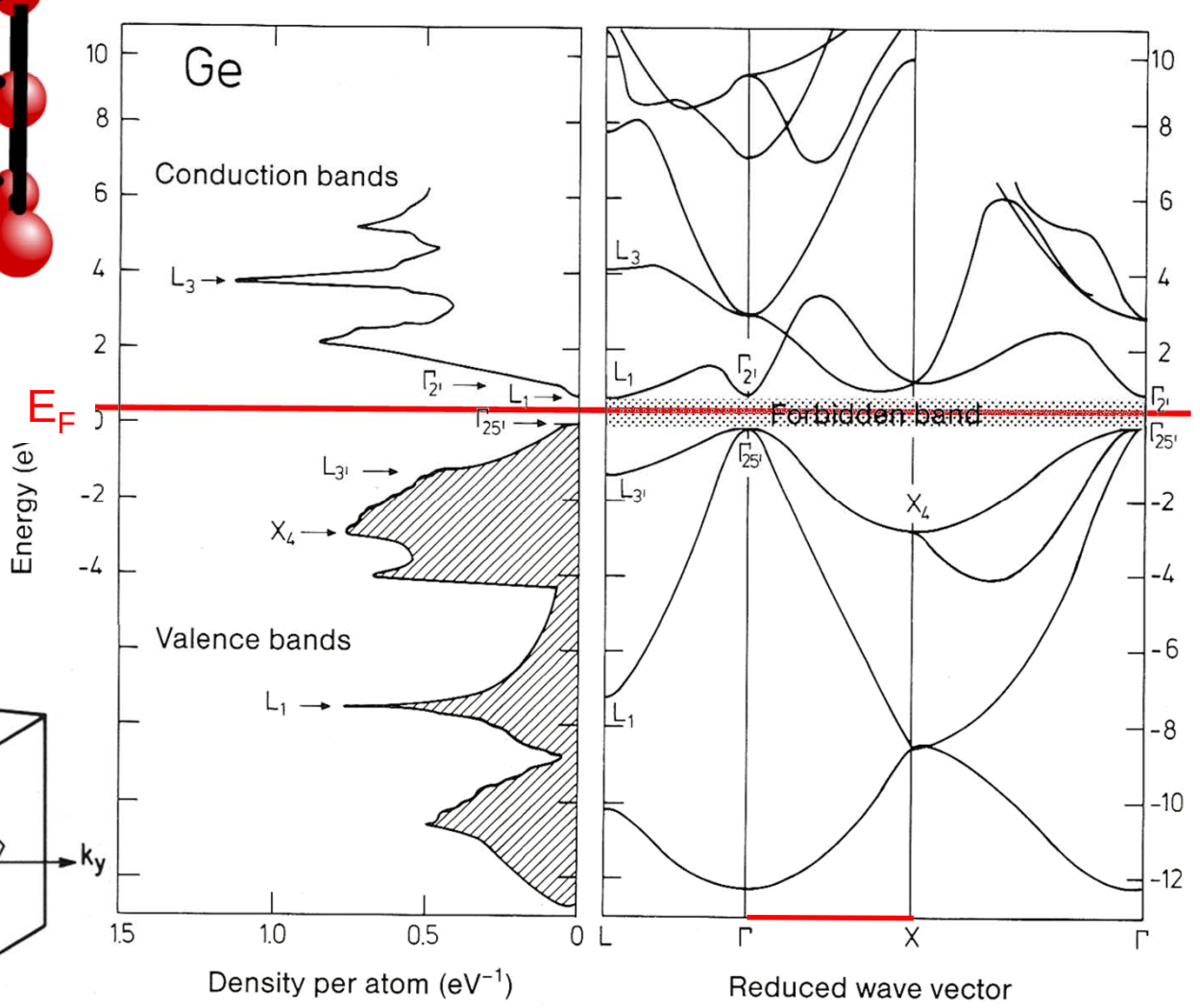

Anti-Bonding (empty at T = 0)

Bandgap, $E_g \approx 0.7$ eV

Bonding (filled at T = 0)

1st Brillouin zone for the bcc lattice

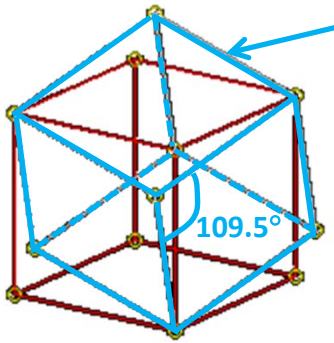

Primitive:

$$\mathbf{a}' = \tfrac{1}{2}a(\hat{\mathbf{x}} + \hat{\mathbf{y}} - \hat{\mathbf{z}})$$
$$\mathbf{b}' = \tfrac{1}{2}a(-\hat{\mathbf{x}} + \hat{\mathbf{y}} + \hat{\mathbf{z}})$$
$$\mathbf{c}' = \tfrac{1}{2}a(\hat{\mathbf{x}} - \hat{\mathbf{y}} + \hat{\mathbf{z}})$$

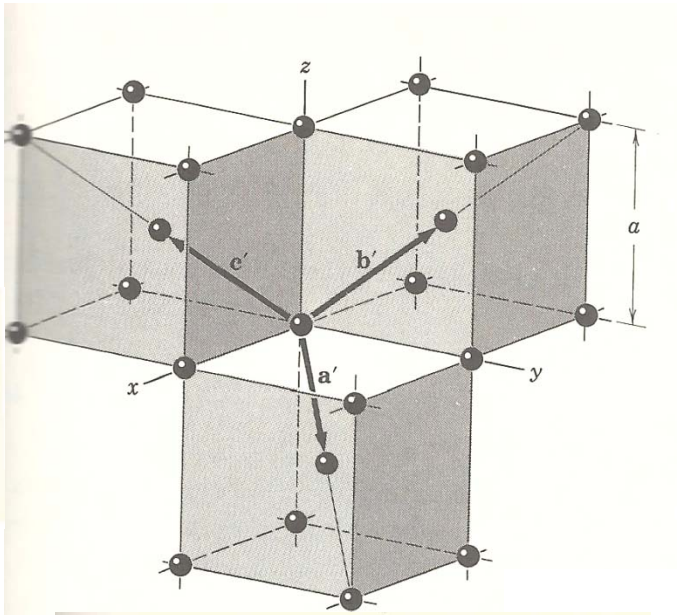

Real bcc

Primitive: Smallest 12

$$\frac{2\pi}{a}(\pm\hat{\mathbf{x}} \pm \hat{\mathbf{y}})$$
$$\frac{2\pi}{a}(\pm\hat{\mathbf{y}} \pm \hat{\mathbf{z}})$$
$$\frac{2\pi}{a}(\pm\hat{\mathbf{x}} \pm \hat{\mathbf{z}})$$

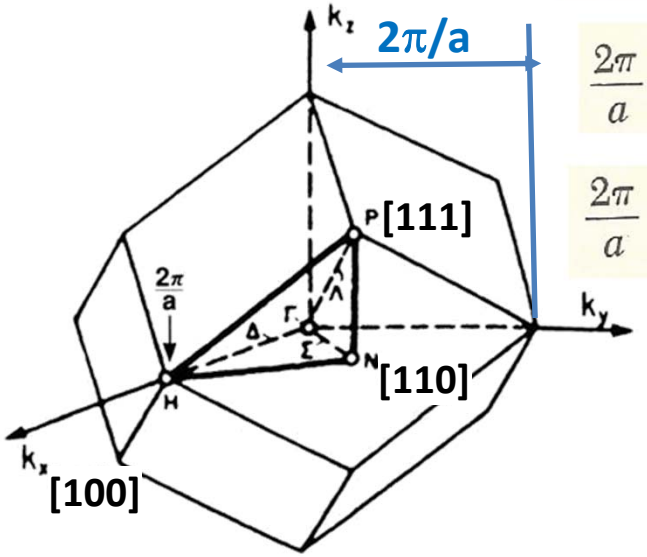

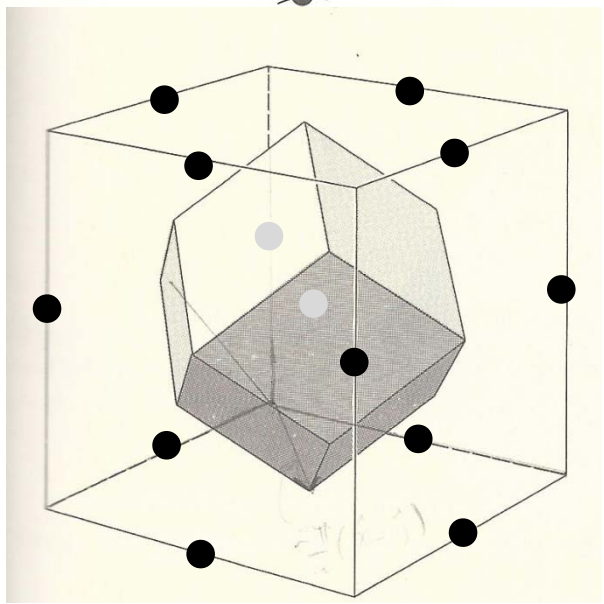

Reciprocal of bcc = fcc

1st Brillouin zone for the bcc lattice

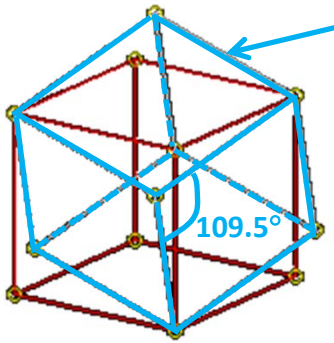

Primitive:

$$\mathbf{a}' = \tfrac{1}{2}a(\hat{\mathbf{x}} + \hat{\mathbf{y}} - \hat{\mathbf{z}})$$
$$\mathbf{b}' = \tfrac{1}{2}a(-\hat{\mathbf{x}} + \hat{\mathbf{y}} + \hat{\mathbf{z}})$$
$$\mathbf{c}' = \tfrac{1}{2}a(\hat{\mathbf{x}} - \hat{\mathbf{y}} + \hat{\mathbf{z}})$$

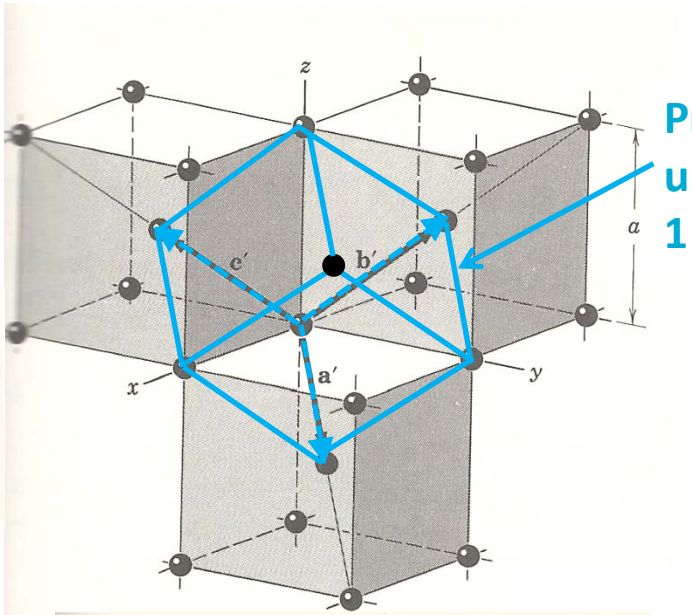

Primitive unit cell: 1 atom

Real bcc

Primitive: Smallest 12

$$\frac{2\pi}{a}(\pm\hat{\mathbf{x}} \pm \hat{\mathbf{y}})$$

$$\frac{2\pi}{a}(\pm\hat{\mathbf{y}} \pm \hat{\mathbf{z}})$$

$$\frac{2\pi}{a}(\pm\hat{\mathbf{x}} \pm \hat{\mathbf{z}})$$

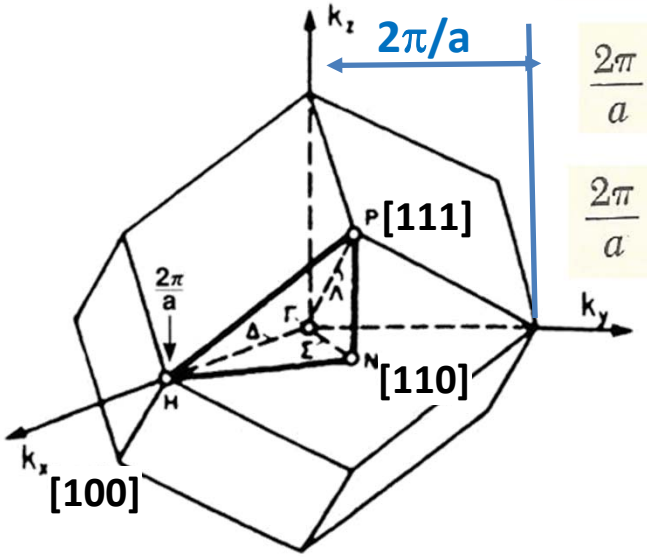

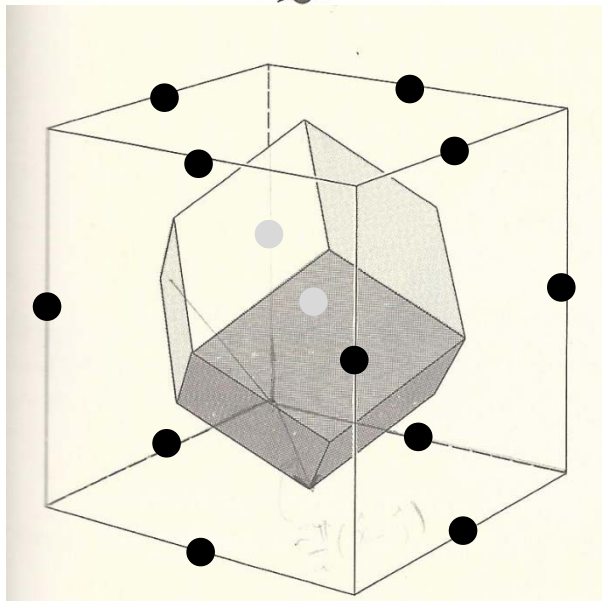

Reciprocal of bcc = fcc

Electronic bands and density of states for a metal-Tungsten—
$1s^2 2s^2\ 2p^6 3s^2 3p^6 3d^{10} 4s^2 4p^6 4d^{10} 5s^2 5p^6 5d^4 6s^2$

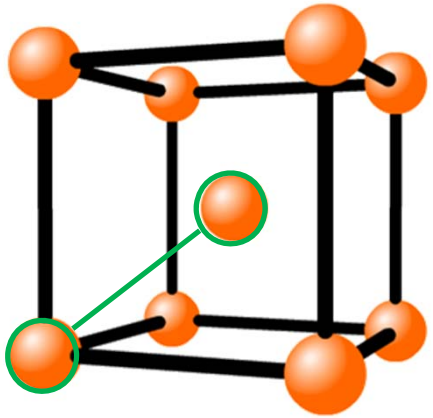

bcc
Simple
cubic
+ 2-atom
basis

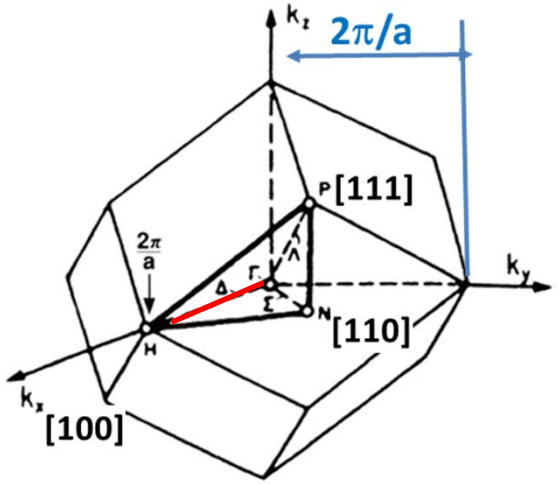

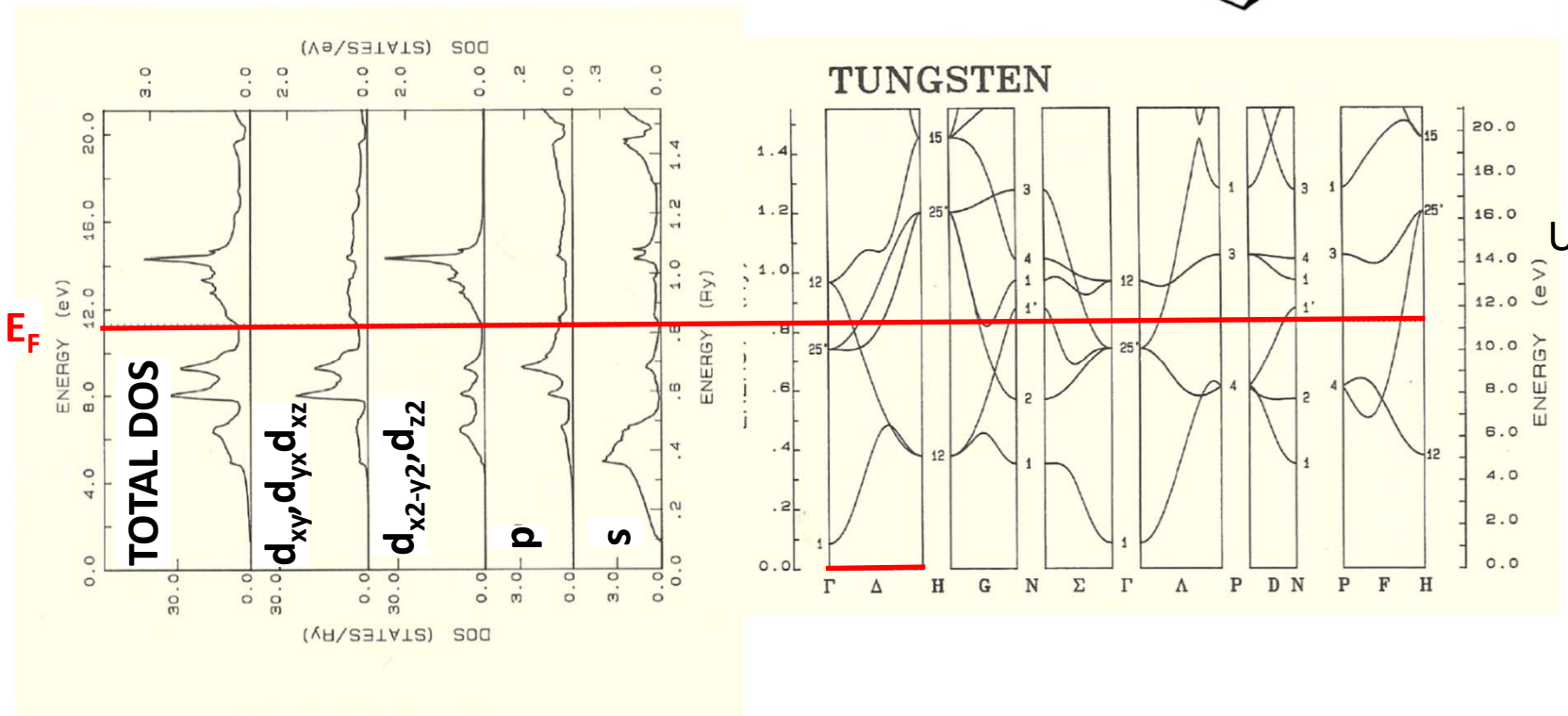

E_F

Unfilled

Filled

Three Brillouin zones

fcc:

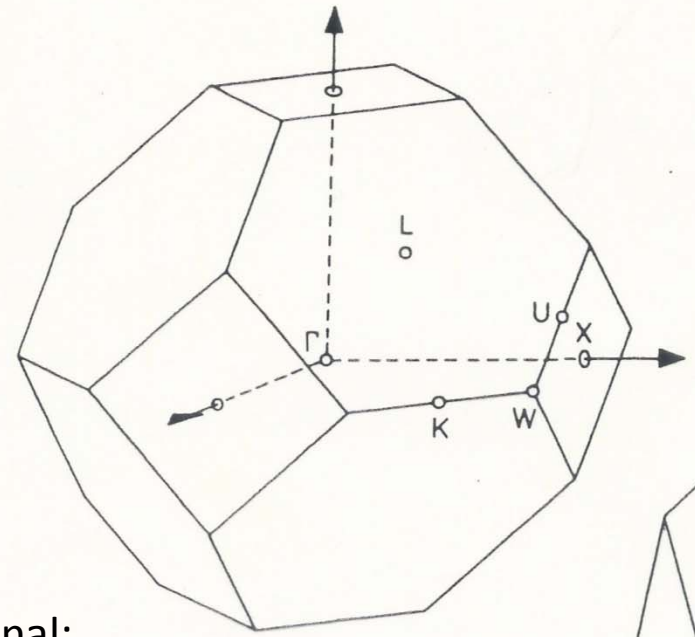

bcc:

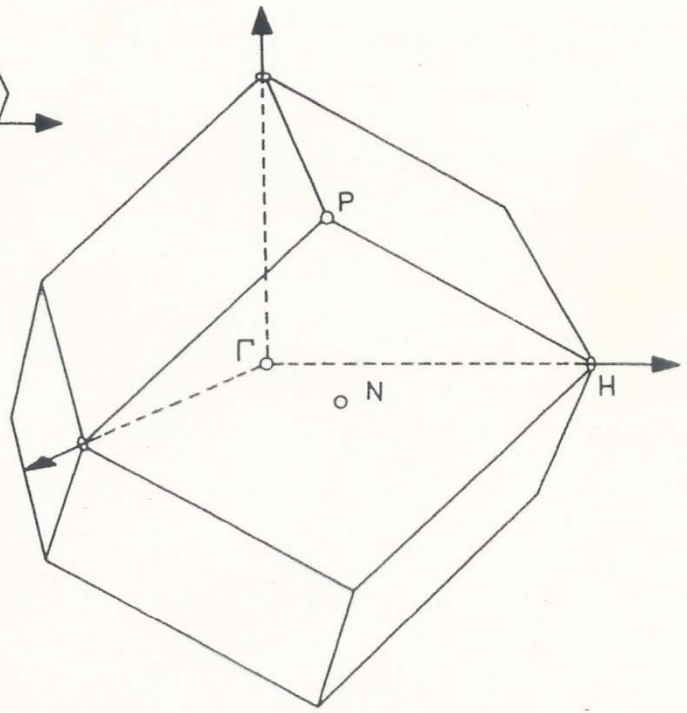

hexagonal:

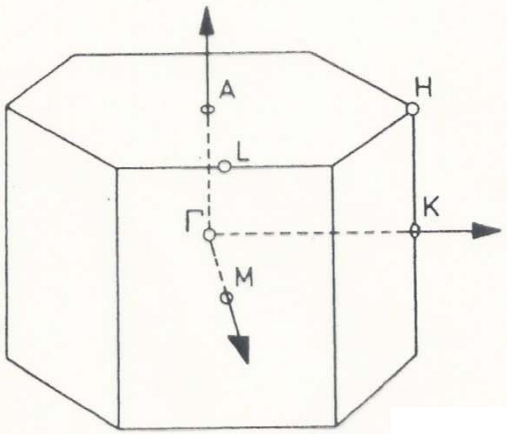

$$\vec{a}_1 = a\hat{x}, \qquad \vec{a}_2 = \tfrac{a}{2}\hat{x} + \tfrac{\sqrt{3}a}{2}\hat{y}, \qquad \vec{a}_3 = c\hat{z}$$

$$\vec{b}_1 = \tfrac{2\pi}{\sqrt{3}a}(\sqrt{3}\hat{k}_x - \hat{k}_y), \qquad \vec{b}_2 = \tfrac{4\pi}{\sqrt{3}a}\hat{k}_y, \qquad \vec{b}_3 = \tfrac{2\pi}{c}\hat{k}_z$$

Some diffracting waves/de Broglie waves

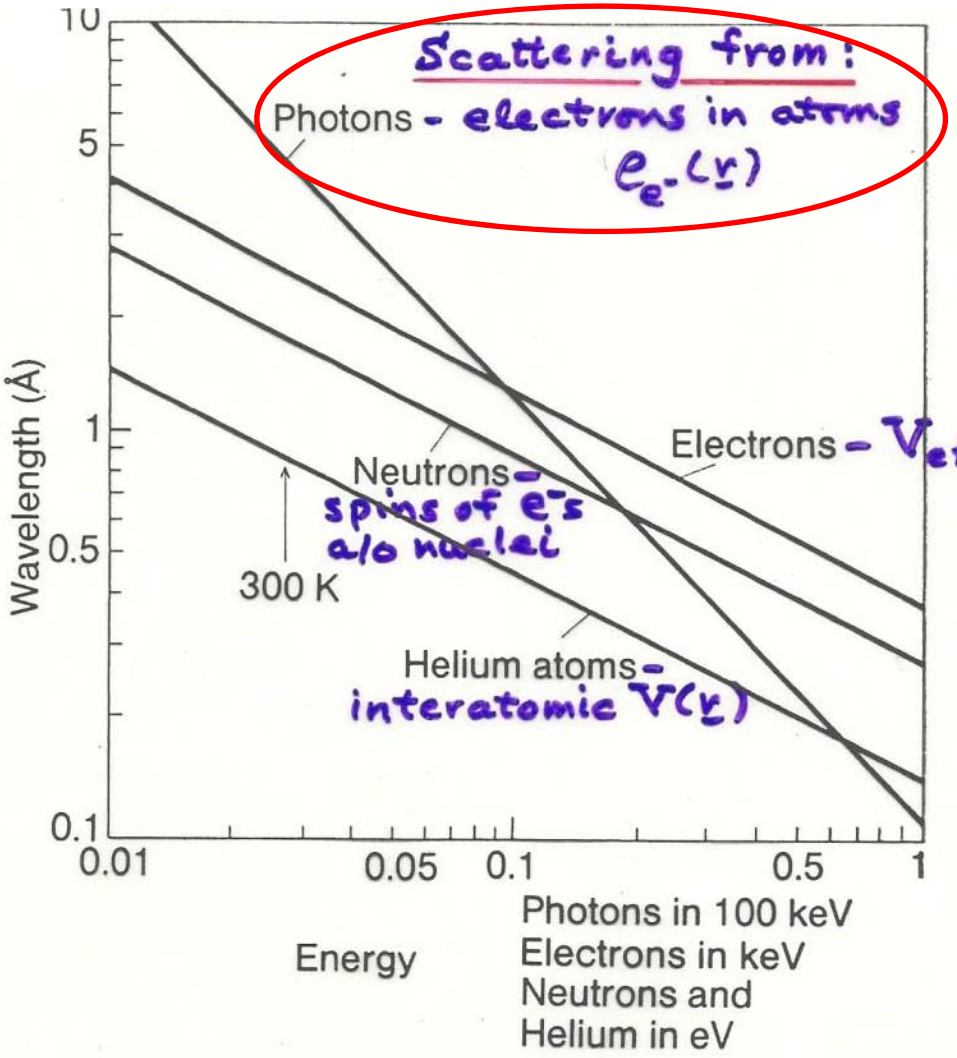

$$\lambda_x = \frac{12{,}400}{h\nu\ (eV)}$$

$$\lambda_e = \frac{h}{p} = \frac{h}{\sqrt{2 m_e E_{kin}}} = \sqrt{\frac{150}{E_{kin}\ (eV)}}$$

$$\lambda_n = \frac{h}{p} = \frac{0.28}{\sqrt{E_{kin}\ (eV)}}$$

$$\lambda_{He} = \frac{h}{p} = \frac{0.14}{\sqrt{E_{kin}\ (eV)}}$$

The Laue Method

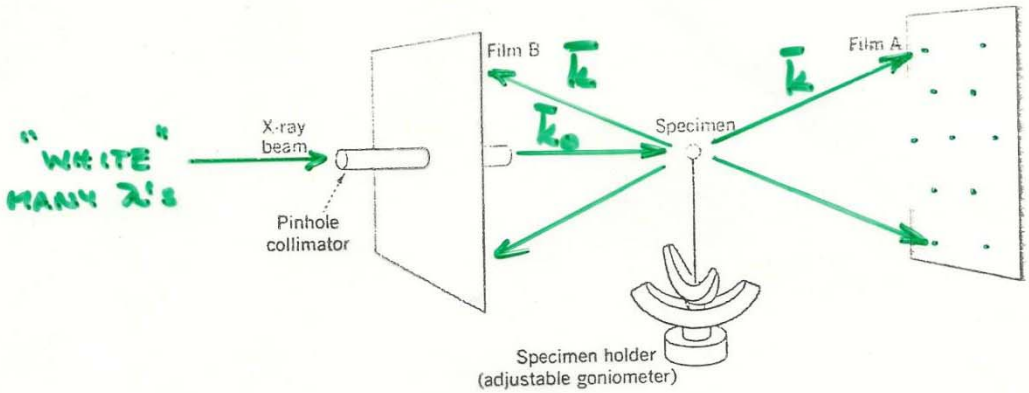

Figure 4 (*above*) A flat plate camera. With a continuous spectrum x-ray beam and a single crystal specimen, the camera produces Laue patterns. The adjustable mount is convenient for the orientation of single crystals, as is often needed in other solid state experiments. The film B is used for back-reflection Laue patterns. (Courtesy of Philips Electronic Instruments.)

Figure 5 (*right*) Laue pattern of a silicon crystal in approximately the [100] orientation. Note that the pattern is nearly invariant under a rotation of $2\pi/4$. The invariance follows from the four-fold symmetry of silicon about a [100] axis. The black center is a cut-out in the film. (Courtesy of J. Washburn.)

The Powder (Debye-Sherrer) Method

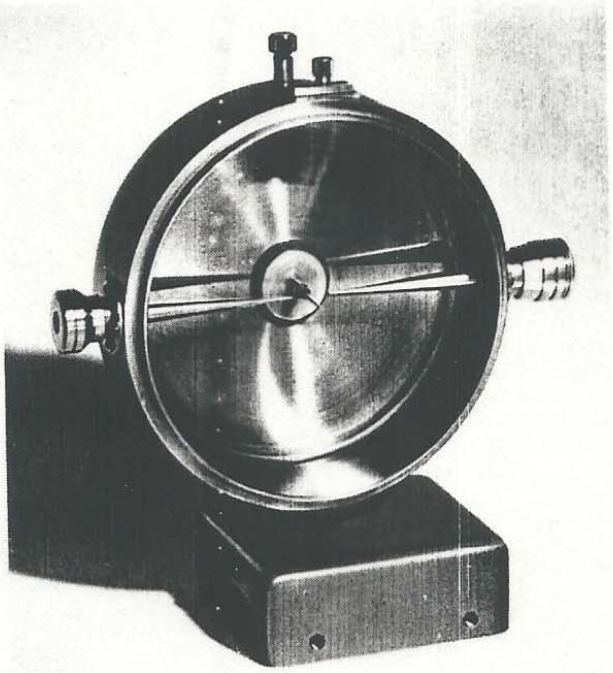

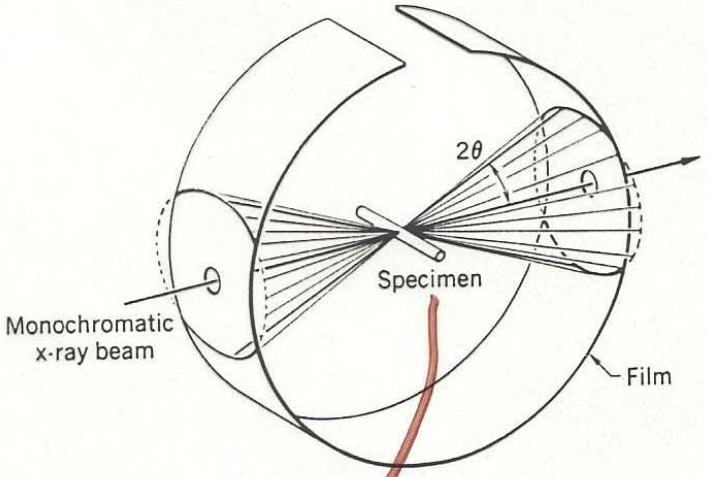

Figure 10 X-ray powder diffraction camera. The specimen is a polycrystalline powder. (Courtesy of Philips Electronic Instruments.)

MANY SMALL CRYSTALLITES RANDOMLY ORIENTED W.R.T. ONE ANOTHER

Low Energy Electron Diffraction (Davisson-Germer revisited)

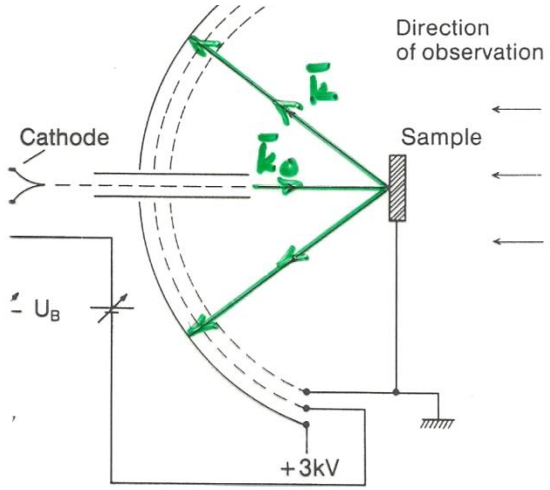

I.1. Schematic of the experimental arrangement used to erve LEED reflections from the surface of a single crystal

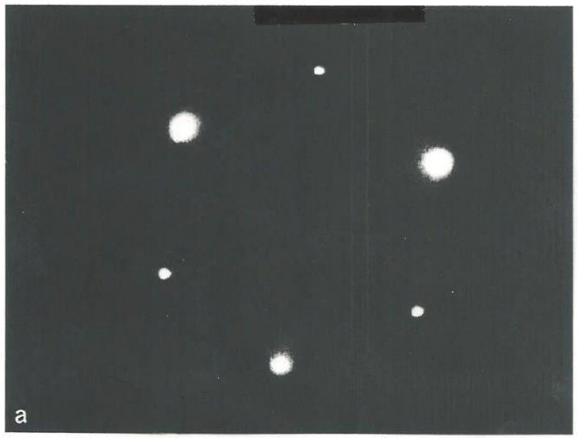

Fig. I.2a. LEED diffraction pattern from a Ni (111) surface at a primary electron energy of 205 eV, corresponding to a wavelength of 0.86 Å. The position of the spots can be used to determine the lattice constant. Of perhaps greater interest are adsorption experiments since adsorbates often form a variety of overlayer structures

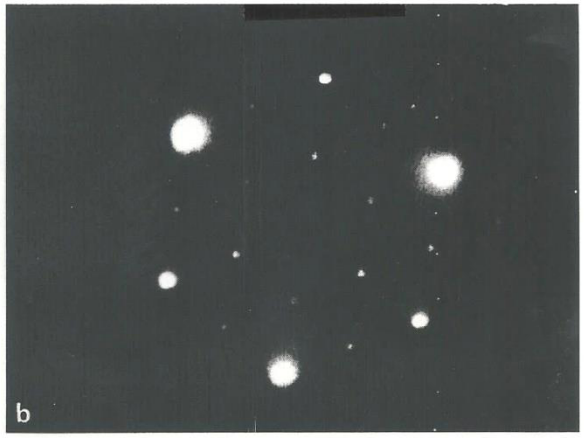

Fig. I.2b. The diffraction pattern observed after the adsorption of hydrogen. The extra spots indicate the formation of a so-called (2×2) adsorbate superstructure, i.e., the elementary mesh of the adsorbate structure is, in both directions, twice as large as that of the nickel substrate

Neutron Diffraction

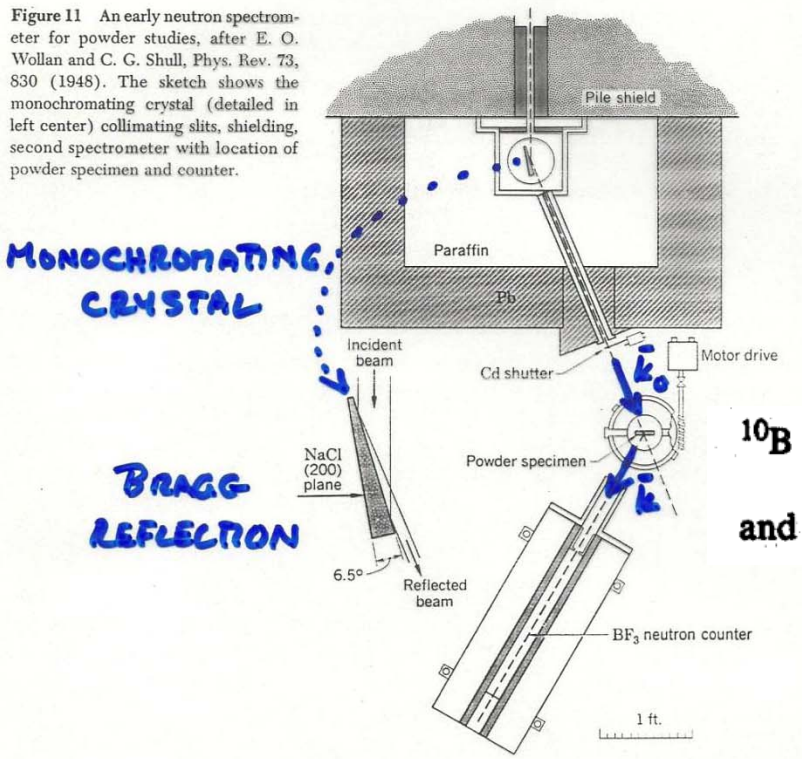

Figure 11 An early neutron spectrometer for powder studies, after E. O. Wollan and C. G. Shull, Phys. Rev. 73, 830 (1948). The sketch shows the monochromating crystal (detailed in left center) collimating slits, shielding, second spectrometer with location of powder specimen and counter.

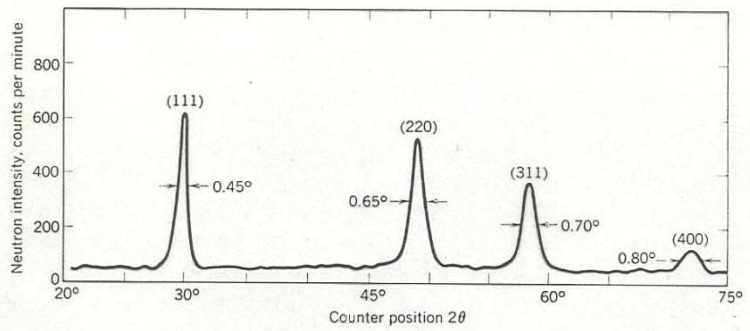

Figure 12 Neutron diffraction pattern for powdered diamond. (After G. Bacon.)

BF_3 detection gas:

$$^{10}B + n \rightarrow {}^{7}Li^{*} + {}^{4}He + 2310\ keV$$

$$\text{and } {}^{7}Li^{*} \rightarrow {}^{7}Li + 480\ keV \quad .$$

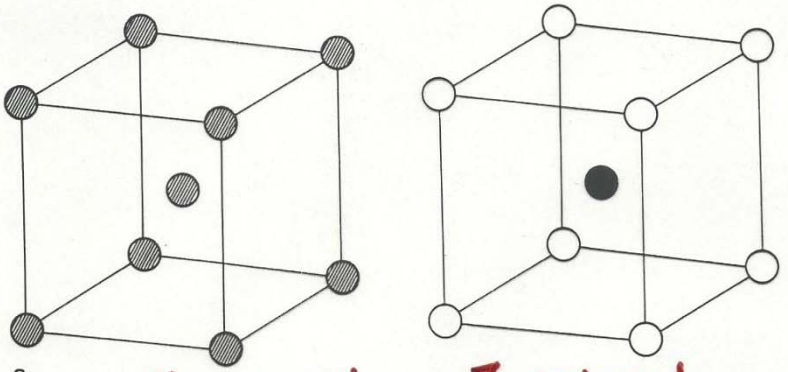

Forbidden (neutron) reflections

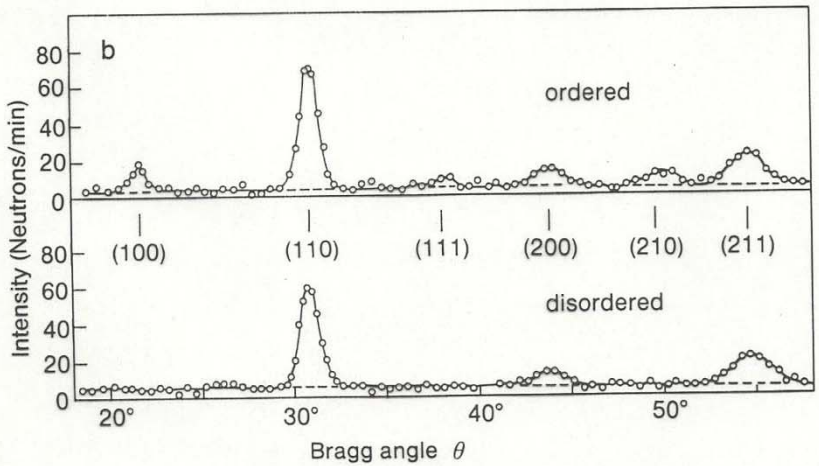

Fig. I.5a. The disordered and ordered phases of FeCo. **b** Neutron diffractogram of the ordered and disordered phases; after [I.6]. Note the low count rates which are typical for neutron diffraction experiments. To obtain good statistics it is necessary t measure for long periods of time

Helium-Atom diffraction

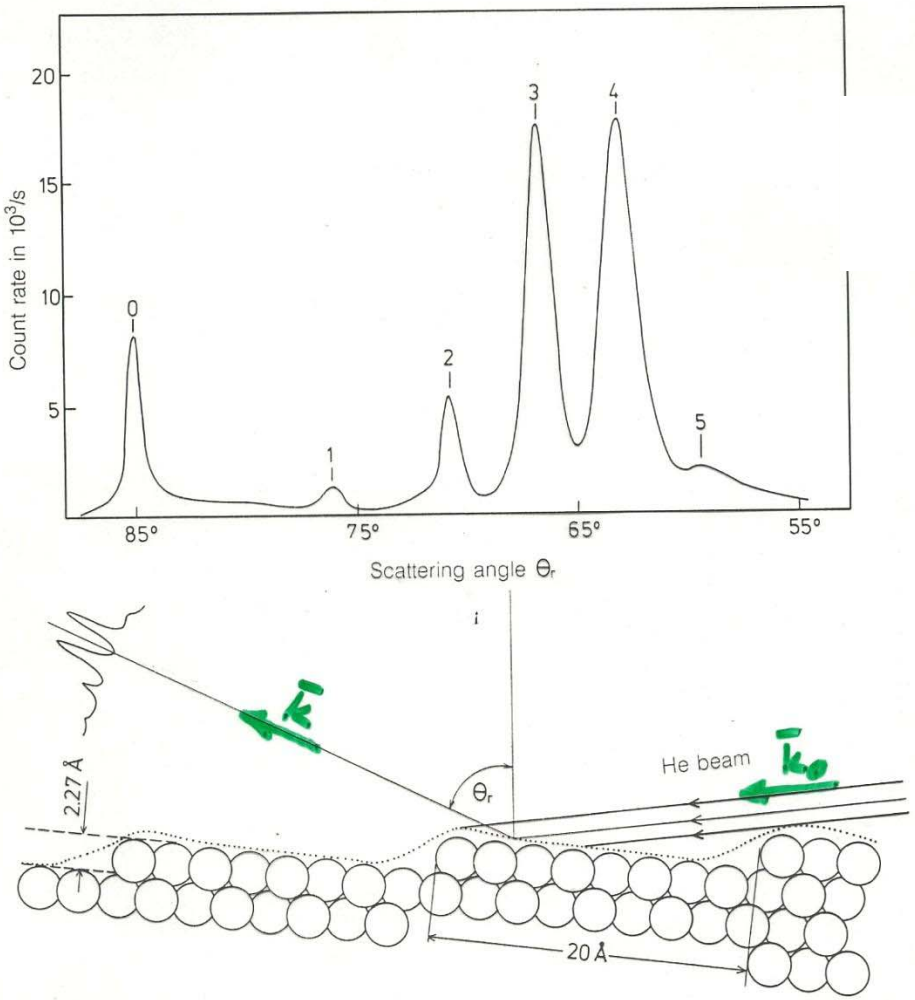

Fig. I.3. Diffraction of a He beam from a stepped platinum surface [I.3]. The Miller indices of this surface are (997). As for an optical echelon, one obtains maximum intensity in the diffraction orders that correspond to specular reflection from the contours of the interaction potential. In this case it should be noted that these potential contours are not exactly parallel to the terraces

Diffraction from a liquid

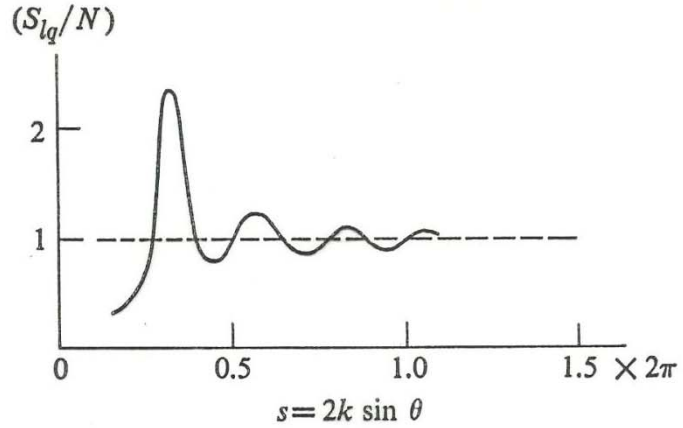

Fig. 2.12 The structure factor for liquid mercury (after Guinier)

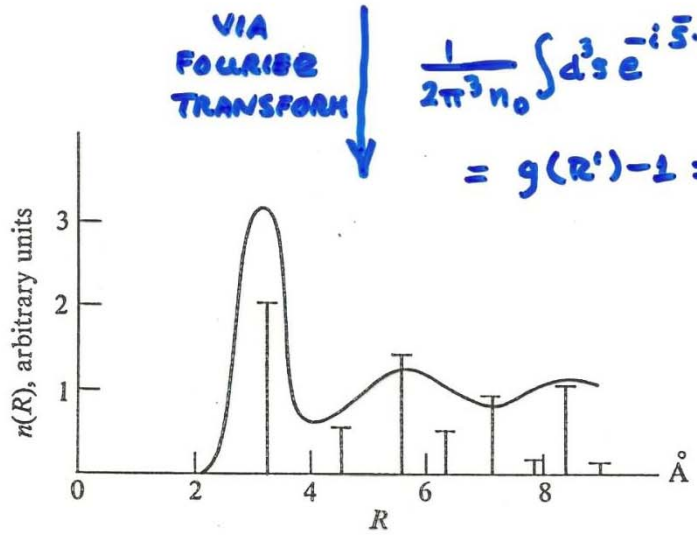

Fig. 1.17 The atomic concentration $n(R)$ in liquid mercury. Vertical line the atomic distribution in crystalline mercury.

Scattering from a single atom: spherically symmetric charge distribution

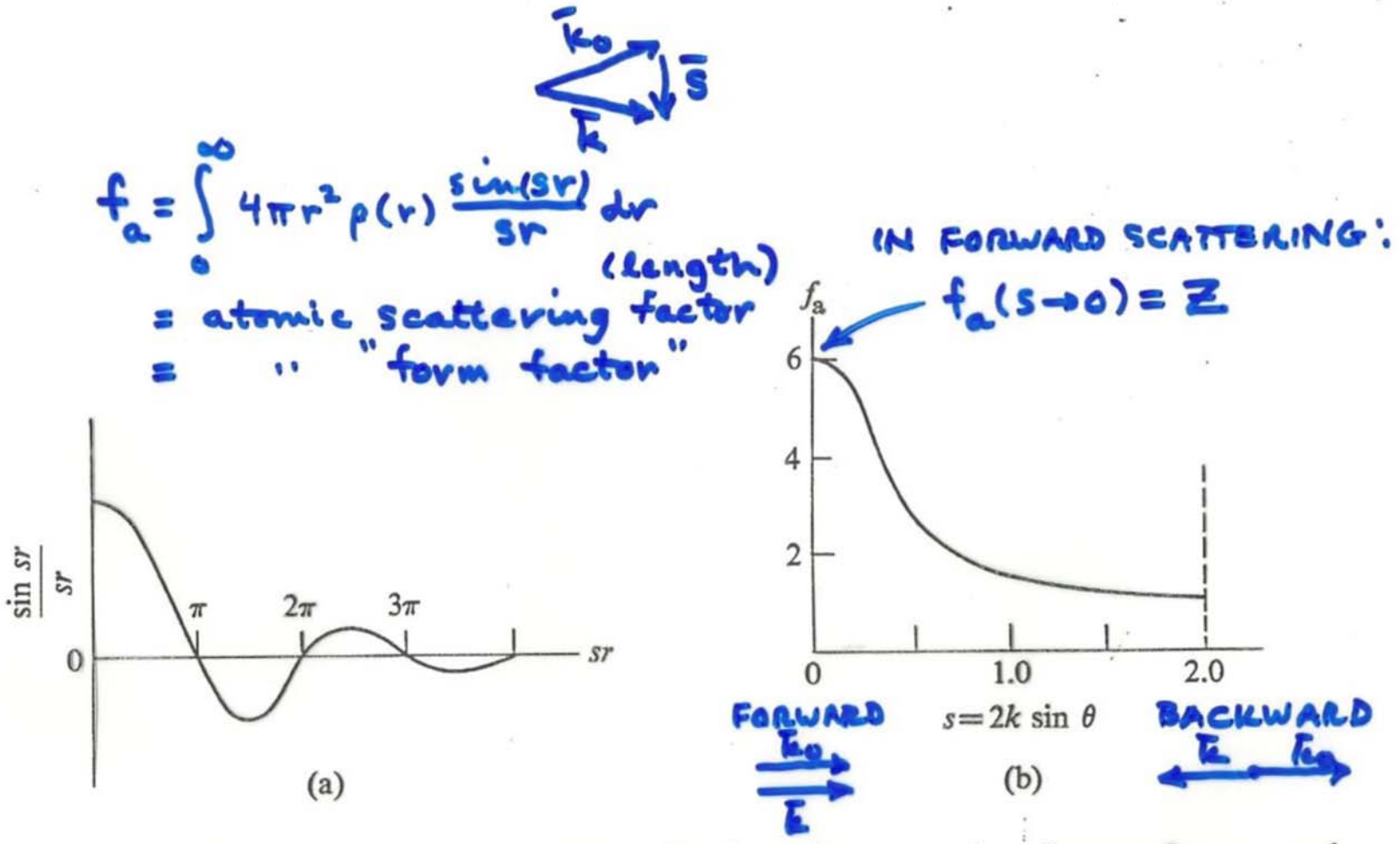

Fig. 2.4 (a) Oscillating factor $\sin(sr)/sr$. (b) Atomic scattering factor for a carbon atom as a function of the scattering angle (after Woolfson).

The shell structure of an Ar atom, as measured and calculated from the Fourier transform of electron diffraction data

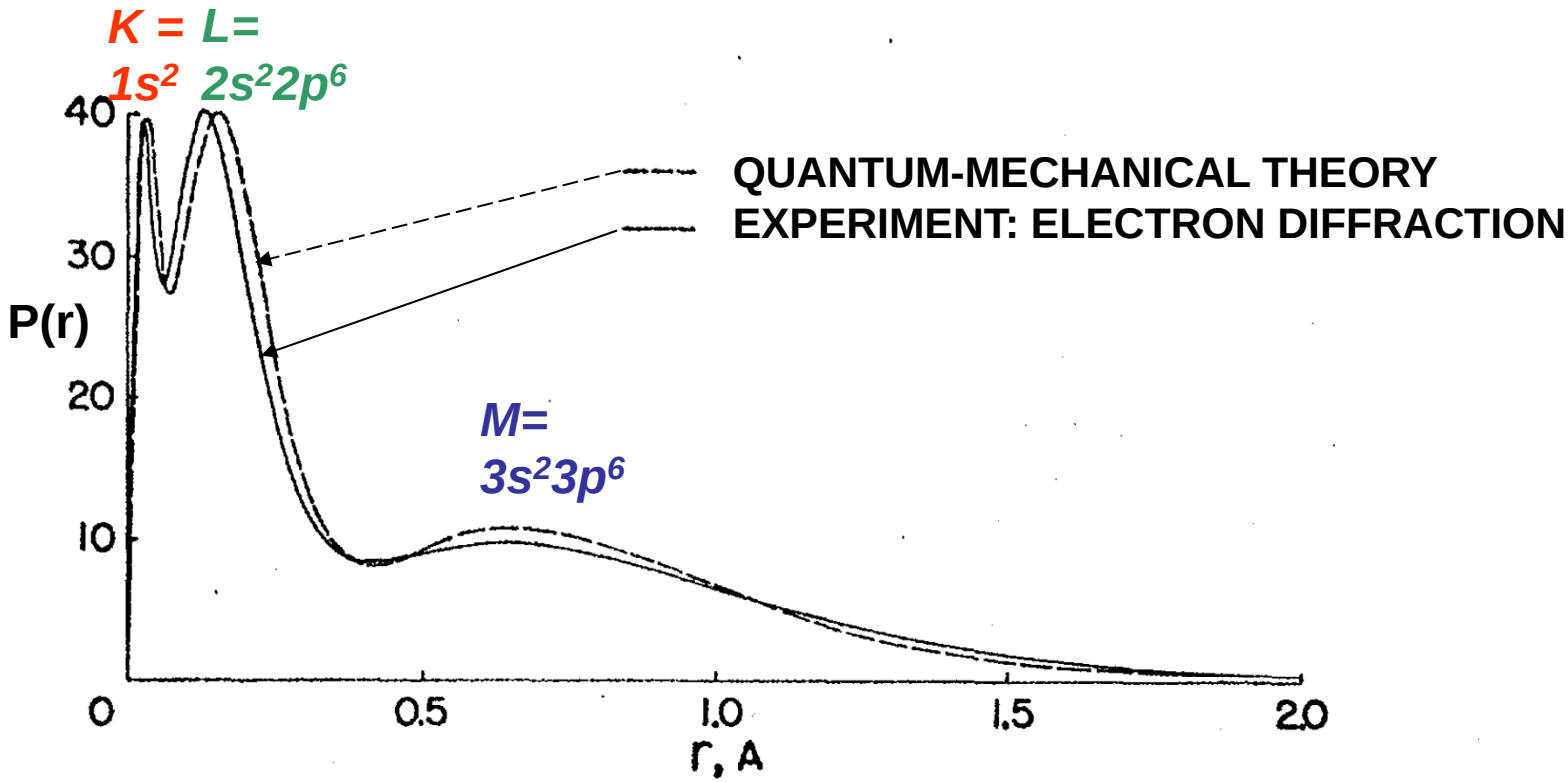

The radial probability distribution of all of the electrons in Argon, as derived from electron diffraction experiments and quantum-mechanical theory

Back to solids: Vibrational effects on diffraction: the Debye-Waller factor

Vibrations smear positions, decrease diffraction→phonons

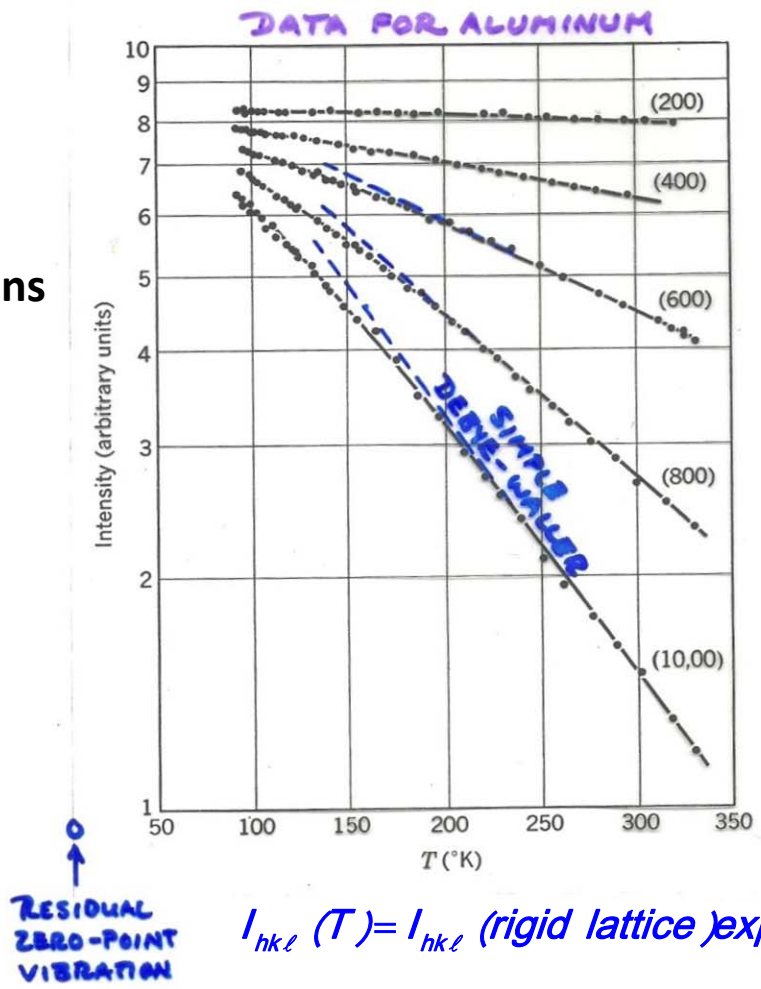

See supplementary reading from Kittel on Debye-Waller factor

$$I_{hk\ell}(T) = I_{hk\ell}(\text{rigid lattice}) \exp\left[-\frac{1}{3} < u^2 > G^2_{hk\ell}\right],$$

if harmonic oscillator with mass M and frequency $\omega = \sqrt{\frac{k}{M}}$,

$$= I_{hk\ell}(\text{rigid lattice}) \exp\left[\frac{-k_B T G^2_{hk\ell}}{M\omega^2}\right]$$